Phosphine-NHC-Phosphonium Ylide Pincer Ligand: Complexation with Pd(II) and Unconventional P-Coordination of the Ylide Moiety

Mohammad Ameskal, Rachid Taakili, Ekaterina S Gulyaeva, Carine Duhayon, Jérémy Willot, Noël Lugan, Christine Lepetit, Dmitry A. Valyaev, Yves Canac

Phosphine-NHC-Phosphonium Ylide Pincer Ligand: Complexation with Pd(II) and Unconventional *P*-Coordination of the Ylide Moiety

Mohammad Ameskal,[†] Rachid Taakili,[†] Ekaterina S. Gulyaeva,[†,‡] Carine Duhayon,[†] Jérémy Willot,[†] Noël Lugan,[†] Christine Lepetit,[†] Dmitry A. Valyaev[†,*] and Yves Canac[†,*]

[†] LCC–CNRS, Université de Toulouse, CNRS, 205 route de Narbonne 31077 Toulouse cedex 4, France

[‡] A. N. Nesmeyanov Institute of Organoelement Compounds (INEOS), Russian Academy of Sciences, 28/1 Vavilov str., GSP-1, B-334, Moscow, 119334, Russia

ABSTRACT: An efficient synthesis of two pincer pre-ligands $[Ph_2PCH(R)ImCH_2CH_2CH_2PPh_3]X_2$ (R = H, X = OTf; R = Ph, X = BF_4) was developed. Subsequent reactions with $PdCl_2$ and an excess of Cs_2CO_3 lead to the formation of highly stable cationic *ortho*-metalated Pd(II) complexes [(*P*,*C*,*C*,*C*)Pd]X exhibiting phosphine, NHC, phosphonium ylide and σ-aryl donor extremities. The protonation of one of the latter complexes with R = H affords the Pd(II) complex $[(P,C,C)Pd(MeCN)](OTf)_2$ bearing an unprecedented nonsymmetrical NHC core pincer scaffold with a 5,6-chelating framework. The overall donor properties of this phosphine-NHC-phosphonium ylide ligand were estimated using experimental ν_{CN} stretching frequency in the corresponding $[(P,C,C)Pd(CN\textit{t}Bu](OTf)_2$ derivative and was shown to be competitive with related bis(NHC)-phosphonium ylide and phenoxy-NHC-phosphonium ylide pincers. The presence of a phenyl substituent in the bridge between phosphine and NHC moieties in *ortho*-metalated complex $[(P,C,C,C)Pd](BF_4)$ makes possible the deprotonation of this position using LDA to provide a persistent zwitterionic complex [(*P*,*C*,*C*,*C*)Pd] featuring a rare *P*-coordinated phosphonium ylide moiety in addition to a conventional *C*-coordinated one. The comparison of the ^{31}P and ^{13}C NMR data for these *C*- and *P*-bound phosphonium ylide fragments within the same molecule was performed for the first time and the bonding situation in both cases was studied in detail by QTAIM and ELF topological analyses.

INTRODUCTION

The growing interest in pincer complexes can be mainly attributed to their stability and structural variability,[1] thus making these metal species essential today in various fields such as homogeneous catalysis,[2] biological systems[3] and functional materials.[4] Historically, the first pincers were prepared in the late 1970's based on an anionic central phenyl ring bearing two neutral pendant phosphine[5] or amine[6] donors. Subsequently, a large variety of pincer systems was designed by modifying the nature of donor atoms, backbone structure and/or auxiliary ligands on the metal center. Among all these assemblies, the most common contain two symmetrical five-membered metallacycles with two similar donor groups.[7] To a lesser extent, symmetrical pincers based on two identical six-membered metallacycles have also been widely considered,[8] showing in some cases better performances in terms of catalytic activity than their smaller 5,5-counterparts due to a greater flexibility.[9] In contrast, nonsymmetrical pincer complexes[10] are not as numerous mainly due to synthetic issues, although they present several potential advantages over their symmetrical analogues such as a greater ability to electronically and sterically tune the coordination sphere of metal, and introduce hemilability and metal-ligand cooperativity. In this category, few nonsymmetrical pincers possessing 5,6-metallacycles have been reported so far,[11] and it has been shown that they can exhibit similar properties as their symmetrical analogues while maintaining their own characteristics and reactivities. For instance, a change in the size of metallacycle modifies ligand bite angle and inevitably influences chemical behavior of corresponding pincer complexes.[12]

Over the years, due mainly to their strong σ-donor ability, the incorporation of NHC fragments within pincer systems has been shown to be beneficial, improving efficiency and selectivity of metal complexation, with a particular emphasis on their catalytic potential.[13] A large number of NHC-based pincers with different sized metallacycles and donor ends was thus reported with the carbene moiety being situated as side arm donors[14] or in the central position of the ligand architecture.[15] In this research area, we have recently prepared a series of pincer Pd(II) complexes **A**-**C** bearing NHC core phosphonium ylide ligands, in which the third end can be a phosphonium ylide,[16] a NHC, or a phenolate (Scheme 1).[17] The electron-rich character of these NHC core pincer ligands enabled the stabilization of Pd(II)−CO adducts[16,17] and was found to have a beneficial effect in catalytic aldehyde allylation with Bu_3Sn(allyl).[17] From a synthetic point of view, they were in most cases obtained by acidic cleavage of the $Pd-C_{aryl}$ bond of a $^{+}P-C_6H_5$ substituent in *ortho*-metalated precursors obtained from readily available N-phosphonioimidazolium salts.[18] The common feature of all these pincer systems rests in the presence of two flexible fused six-membered palladacycles with two lateral coordinating extremities connected to central NHC unit. With the aim of introducing more diversity in such carbon-based pincer platforms, we report herein the preparation of nonsymmetrical 5,6-NHC core pincer Pd(II) complexes of type **D** featuring phosphonium ylide and phosphine donor moieties. In addition, thanks to the possible tuning of lateral phosphine arm, we were able to prepare and characterize complex **E** combining regular *C*-coordinated phosphonium ylide[19] with a rare *P*-pallada-substituted ylide moiety.[20]

Scheme 1. Previously Reported 6,6-NHC Core, Phosphonium Ylide-Containing Pincer Pd(II) Complexes A-C, and Targeted Pd(II) Compounds D-E Derived from 5,6-Phosphine-NHC-Phosphonium Ylide Scaffold.

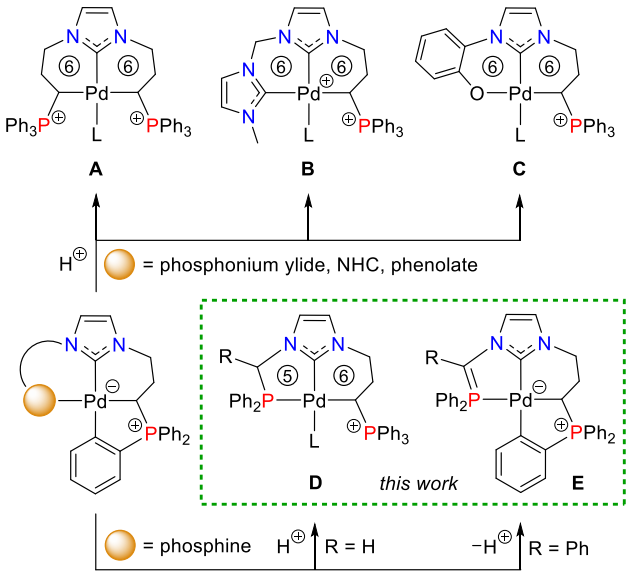

RESULTS AND DISCUSSION

Synthesis and Spectroscopic Characterization of Phosphine-NHC-Phosphonium Ylide Pre-Ligand $[Ph_2PCH_2Im(CH_2)_3PPh_3](OTf)_2$ and Its Pd(II) Complexes. In order to introduce a phosphonium arm to a NHC core pincer scaffold, the *N*-phosphine oxide substituted imidazole **1**[11f] was first reacted with commercially available (3-bromopropyl)triphenylphosphonium bromide in DMF at 120°C (Scheme 2). The resulting *N*-phosphonioimidazolium salt [**2**]Br_2 was thus isolated in 95% yield, and its exact structure was unambiguously confirmed by single crystal X-ray diffraction (Figure S32).[21] Subsequent reduction of the phosphine oxide moiety was achieved by heating [**2**]Br_2 with an excess of $PhSiH_3$ in chlorobenzene at 120°C in the presence of bis(4-nitrophenyl)phosphate as organocatalyst.[22] To our delight, we observed that under these conditions the phosphonium fragment remains intact, and after Br/OTf anion exchange the desired imidazolium salt [**3**]$(OTf)_2$ was obtained in almost quantitative yield. The ^{31}P NMR spectrum of [**3**]$(OTf)_2$ displayed two singlet signals at δ_P 24.0 and −12.6 ppm, in the normal range for $-^{+}PPh_3$ and $-PPh_2$ fragments, respectively, being in the latter case different to those of phosphine oxide precursor [**2**]Br_2 (δ_P 26.1 and 24.4 ppm for $-P(O)Ph_2$ and $-^{+}PPh_3$ moieties). As expected, ^1H NMR signal of N_2CH fragment in [**3**]$(OTf)_2$ (δ_H 8.96 ppm) was deshielded related to that of neutral precursor 1 (δ_H 7.30 ppm). According to the conditions developed in related systems,[16a,17] the coordination of salt [**3**]$(OTf)_2$ was achieved in an one-pot procedure by adding a stoichiometric amount of $PdCl_2$ and an excess of cesium carbonate in MeCN at 50°C (Scheme 3). Following initial coordination of the phosphine arm and sequential base-assisted activation of three C−H bonds, the *ortho*-metalated Pd(II) complex [**4**](OTf) was obtained in 74% yield. The high stability of [**4**](OTf) with respect to air and moisture allowed its purification by chromatography on silica. The identity of complex [**4**](OTf) was first proposed on the basis of its ^{31}P NMR data showing two doublets at δ_P 43.3 ppm (d, $^3J_{PP}$ = 16.5 Hz, PPh_2) and 34.4 ppm (d, $^3J_{PP}$ = 16.5 Hz, PPh_2^+),

Scheme 2. Synthesis of Phosphine-Imidazolium-Phosphonium Salt [3](OTf)$_2$ from *N*-Phosphine Oxide Substituted Imidazole 1.

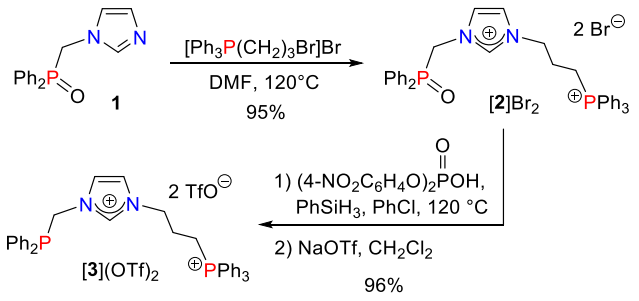

deshielded relative to those of its *N*-phosphonio precursor [**3**]$(OTf)_2$ (δ_P 24.0 ppm (s); −12.6 ppm (s)).The coordination of CH ylide was evidenced by the presence of characteristic high-field ^{13}C NMR doublet of doublets at δ_C 25.4 ppm (dd, $^1J_{CP}$ = 85.1 Hz, $^2J_{CP}$ = 41.3 Hz). The ^{13}C NMR spectrum also unveiled the presence of characteristic signals of *ortho*-metallated carbon atom at δ_C 175.8 ppm (dd, $^2J_{CP}$ = 35.2 and 6.2 Hz) with neighboring C_{ipso} atom at δ_C 139.3 ppm (d, $^1J_{CP}$ = 117.6 Hz) as well as NHC resonance at δ_C 178.8 ppm (dd, J_{CP} = 12.1 and 6.3 Hz). ESI mass spectroscopy data (*m/z* 673.1 $[M - OTf]^+$) unambiguously confirmed the cationic nature of [**4**](OTf). The molecular structure of [**4**](OTf) was determined by X-ray diffraction (*vide infra*).[21]

Scheme 3. Sequential Synthesis of Phosphine-NHC-Phosphonium Ylide Pd(II) Pincer Complexes [5](OTf)$_2$ and [6](OTf)$_2$ from Imidazolium Salt [3](OTf)$_2$.

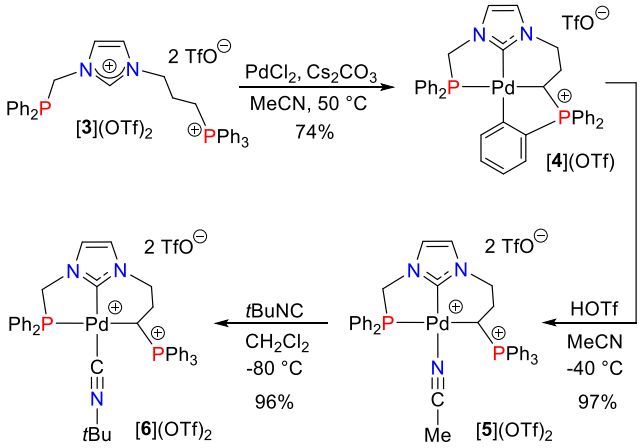

The desired 5,6-pincer complex [**5**]$(OTf)_2$ was obtained in 97% yield by the protonation of [**4**](OTf) with one equivalent of TfOH in MeCN at low temperature leading selectively to the cleavage of Pd−C_{aryl} bond of the *ortho*-phenylated ring. ^{31}P NMR spectrum of complex [**5**]$(OTf)_2$ contains two doublets at relatively high field (δ_P 42.4 ppm (d, $^3J_{PP}$ = 2.4 Hz, PPh_2) and δ_P 31.0 ppm (d, $^3J_{PP}$ = 2.4 Hz, PPh_3^+), slightly modified with respect to its *ortho*-metalated Pd(II) precursor [**4**](OTf). In addition, the persistence of Pd−ylidic bond was evidenced by the presence of high-field doublet of doublets signal (δ_{CH} 14.6 ppm, dd, $^1J_{CP}$ = 95.6 Hz, $^2J_{CP}$ = 30.1 Hz) in ^{13}C NMR spectrum. Upon [**4**](OTf) → [**5**]$(OTf)_2$ transformation the carbene signal was shifted upfield by *ca.* 20 ppm and lost the coupling with one of phosphorus atoms (δ_C 178.8 ppm (dd, J_{CP} = 12.1 and 6.3 Hz) *vs.* 156.8 ppm (d, J_{CP} = 7.0 Hz)). To evaluate the overall electronic donation of this novel *P,C,C*-pincer ligand, the substitution of

MeCN ligand with *t*-butylisocyanide was then performed in CH_2Cl_2 at −80°C, leading to the corresponding adduct [**6**](OTf)$_2$ in 96% yield (Scheme 3). While the position of ^{31}P NMR signals of [**6**](OTf)$_2$ remained essentially unchanged (δ_P 45.5 and 34.2 ppm) compared to those of its precursor [**5**](OTf)$_2$ the expected $^3J_{PP}$ coupling constant was not observed in this case. The presence of isocyanide ligand was confirmed by IR ($\nu_{C\equiv N}$ at 2206 cm^{-1} in CH_2Cl_2) and ^{13}C NMR spectroscopy by the broad signal at δ_C 132.0 ppm of the coordinated carbon atom along with two other characteristic resonances of the *t*Bu group at δ_C 59.5 and 28.8 ppm. Finally, the molecular structure of [**6**](OTf)$_2$ was further confirmed by X-ray diffraction (*vide infra*).[21] The comparison of experimental $\nu_{C\equiv N}$ frequency value for [**6**](OTf)$_2$ with those of complexes [**7**](OTf)$_2$ and [**8**](OTf) (2206–2207 cm^{-1}) revealed that the new 5,6-*P,C,C*-pincer ligand has similar donor character than the related 6,6-membered phosphonium ylide-based analogues exhibiting NHC or phenolate donor extremities (Scheme 4).[17] These values also indicate that only pincer ligands in complexes [**9**](OTf)$_2$ (2194 cm^{-1}) and [**10**](OTf) (2187 cm^{-1}) featuring respectively two peripheral ylides[16a] and a central ylide[23] exhibit greater electronic donation. Given that complexes [**6**](OTf)$_2$ and [**7**](OTf)$_2$ bearing neutral *P,C,C*- and *C,C,C*-pincer ligands respectively, have the same overall charge (+2),[17] the similarity of their electronic properties is rather unexpected taking into account the generally higher donation of NHCs *vs.* aryl-substituted phosphines. However, beyond geometric distortion that may impact overlap of metal/ligand orbitals and given that is the global electronic effect of the pincer ligand which is estimated here, it is possible that the lower phosphine donation is compensated by that of the two carbon extremities, and especially by the strongly σ-donating *trans*-ylide.

Scheme 4. Representative Isocyanide Pd(II) Complexes Bearing Phosphonium Ylide-Based Pincer Ligands and the Corresponding Experimental IR $\nu_{C\equiv N}$ Values.

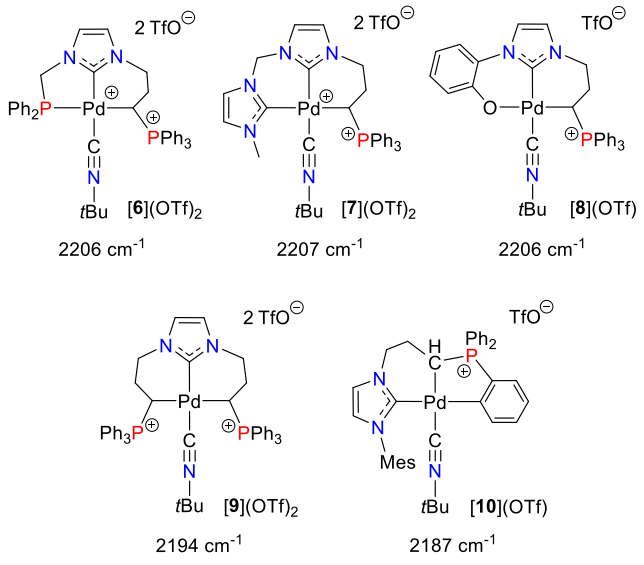

Synthesis and Spectroscopic Characterization of Phosphine-NHC-Phosphonium Ylide Pincer Pre-Ligand [$Ph_2PCHPhIm(CH_2)_3PPh_3$](BF$_4$)$_2$ and its Pd(II) Complexes. In order to introduce structural diversity at the phosphine arm, we have inverted the synthetic strategy used for [**3**](OTf)$_2$ (*vide supra*) starting in this case from *N*-phosphonio-substituted imidazole [**11**](BF$_4$) and electrophilic manganese methylenephosphonium complex [**12**](BF$_4$) (Scheme 5) previously used for metal-mediated assembly of bi- and tridentate NHC-phosphine ligand precursors.[24] Thus, the target pre-ligand [**13**](BF$_4$)$_2$ was isolated in 80% yield by alkylation of [**11**](BF$_4$) with [**12**](BF$_4$) in CH_2Cl_2 at room temperature followed by demetallation under visible light irradiation (Scheme 5).[24,25] The identity of pre-ligand [**13**](BF$_4$)$_2$ was established on the basis of ^{31}P and ^{1}H NMR spectroscopy with the presence of two singlets at δ_P 21.7 and −8.4 ppm for $-^+PPh_3$ and $-PPh_2$ extremities and at δ_H 8.64 ppm for N_2CH proton, respectively.

Scheme 5. Synthesis of Phosphine-Imidazolium-Phosphonium Salt [13](BF$_4$)$_2$ from *N*-Phosphonium Substituted Imidazole [11](BF$_4$).

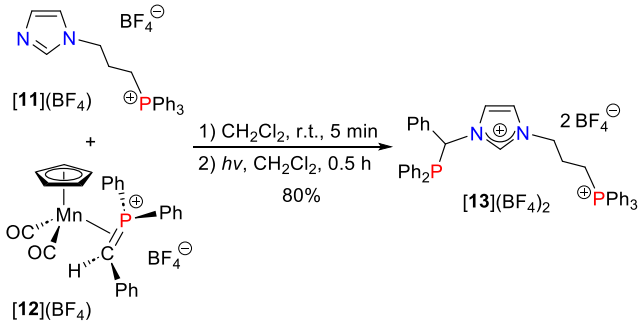

Considering that the phenyl group at the phosphine arm and different counter anion should not significantly impact coordination of [**13**](BF$_4$)$_2$ with Pd(II) center we used the same reaction conditions as for simpler pre-ligand [**3**](OTf)$_2$ ($PdCl_2$, excess of Cs_2CO_3, MeCN, 50 °C). Gratifyingly, the *ortho*-metalated Pd(II) complex [**14**](BF$_4$) was isolated in 69% yield as a mixture of two diastereomers (ratio 70/30), differing by the position of phenyl substituent related to phosphonium moiety at the stereogenic ylidic center (Scheme 6). Both of them display similar spectroscopic features as evidenced in the ^{31}P NMR (major: δ_P 60.3 and 32.1 ppm, d, $^3J_{PP}$ = 17.8 Hz; minor: δ_P 61.3 and 34.9 ppm, d, $^3J_{PP}$ = 16.2 Hz) and ^{13}C NMR spectra for coordinated ylide moieties (major: δ_C 25.8 ppm, dd, $^1J_{PC}$ = 84.8 Hz, $^2J_{PC}$ = 41.4 Hz; minor: δ_C 25.5 ppm, dd, $^1J_{PC}$ = 85.8 Hz, $^2J_{PC}$ = 41.4 Hz). Anticipating that the introduction of phenyl substituent is expected to significantly increase the acidity of the benzylic C–H bond between NHC and phosphine moieties we instead decided to explore the reactivity of [**14**](BF$_4$) towards a base.

After a screening of different bases, it was shown that treatment of complex [**14**](BF$_4$) with an excess of LDA in THF-d_8 at −80 °C give the best compromise affording zwitterionic Pd(II) complex **15** in a spectroscopically quantitative yield (Scheme 6). According to NMR spectroscopy data, complex **15** was found to be relatively unstable in solution at room temperature and therefore its full characterization was achieved at 0 °C. Unlike the precursor [**14**](BF$_4$), ^{31}P NMR spectrum of **15** displays only a single set of doublet signals with two very close resonances (δ_P 29.6 ppm and 30.1 ppm, $^3J_{PP}$ = 14.6 Hz) being consistent with a disappearance of the benzylic stereocenter in the molecule. The ^{31}P NMR resonance of *P*-center directly bonded to metal atom appeared to be strongly shielded compared to those of [**14**](BF$_4$) (δ_P 60.3 and 61.3 ppm), while that of the phosphonium ylide is much less affected (δ_P 32.1 and 34.9 ppm). These ^{31}P NMR values suggest that the environment of coordinated P-atom is significantly modified supporting the deprotonation of CHPh position. The nature of deprotonated species **15** was further assigned with the absence of

Scheme 6. Synthesis of *Ortho*-Metalled NHC, Phosphonium Ylide-Based Pd(II) Complex [14](BF$_4$) and Its Reactivity with LDA.

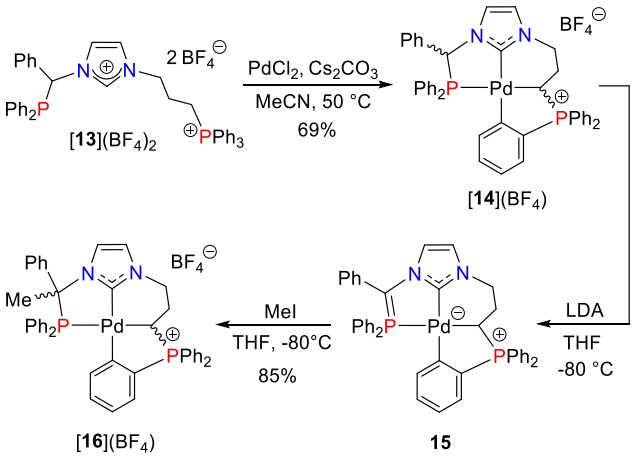

characteristic CH benzylic proton and the appearance of a quaternary carbon atom with adequate multiplicity at δ_C 68.0 ppm (d, $^1J_{PC}$ = 83.1 Hz) in the ^{1}H and ^{13}C NMR spectra, respectively. This signal is significantly downfield compared to that of regular coordinated phosphonium ylide at δ_C 22.6 ppm ($^1J_{PC}$ = 78.5 Hz and $^2J_{PC}$ = 39.3 Hz) in the same metal environment. Finally, two other characteristic ^{13}C NMR signals, for *ortho*-metallated and NHC centers were observed as doublets of doublets at δ_C 181.4 ($^2J_{PC}$ = 34.7 and 6.0 Hz), and 169.4 ppm (J_{PC} = 12.1 and 6.0 Hz), respectively.

In order to unambiguously confirm the acidic site position in [**14**](BF$_4$), complex **15** was treated with a classical alkylating agent such as MeI in THF at low temperature. The resulting Pd(II) complex [**16**](BF$_4$) was obtained in 85% yield as a mixture of two diastereomers (ratio 95/5) as indicated by the presence of four ^{31}P NMR doublet resonances (major: δ_P 76.3 and 32.3 ppm with $^3J_{PP}$ = 17.8 Hz; minor: δ_P 77.1 and 32.6 ppm with $^3J_{PP}$ = 16.2 Hz). Examination of ^{1}H and ^{13}C NMR spectra confirmed that the methylation took place at the bridging carbon position by the observation of the characteristic signal of quaternary carbon atom at δ_C 69.9 ppm (d, $^1J_{CP}$ = 30.3 Hz) and other NMR signals similar to those found in its non-methylated analogue [**14**](BF$_4$). Noteworthy, the decisive role of phenyl substituent was clearly identified since treatment of unsubstituted *ortho*-metalated Pd(II) complex [**4**](OTf) with LDA in THF only led to a mixture of unidentified compounds. Compound **15** represents a unique example of complex combining regular *C*-coordinated phosphonium ylide ligand with a rare *P*-metallasubstituted phosphonium ylide fragment. While the latter species are extremely scarce in literature,[20] it was recently shown by DFT calculations that the related complex *fac*-[(Ph$_2$P=CHNHC)Mn(CO)$_3$] was involved as a key intermediate in cooperative dihydrogen activation.[26] The structure and bonding of **15** was further investigated in detail by theoretical means (*vide infra*).

X-ray Diffraction Studies of Phosphine-NHC-Phosphonium Ylide-Containing Pd(II) Complexes [4](OTf), [6](OTf)$_2$ and [14](BF$_4$). Single-crystal X-ray diffraction studies enabled us to access to the solid state structures of cationic *ortho*-metallated Pd(II) complexes [**4**](OTf) and [**14**](BF$_4$) as well as complex [**6**](OTf)$_2$ exhibiting phosphine-NHC-phosphonium ylide pincer ligand (Figure 1).[21] Selected metrical data for these compounds are gathered in Table 1. Complex [**14**](BF$_4$) exists as two crystallographically independent molecules in the cell having similar metrical data within experimental error except for Pd−P bond distances (2.2736(9) and 2.3130(10) Å). In all complexes, metal atom is situated in a slightly distorted square planar-environment as indicated by τ_4 parameter values of (0.11−0.14).[27] The *ortho*-metalated Pd(II) complexes [**4**](OTf) and [**14**](BF$_4$) differing only by the nature of carbon chain (CH$_2$ *vs.* CHPh) between NHC and phosphine fragments present similar geometric data (Table 1). The P1−C1−C7−C13 plane consists of the phosphine and three carbon donors of different nature belonging to NHC, ylide and *ortho*-phenylated ring, respectively. This specific arrangement results in the formation of highly constraint structures composed of two five-membered and six-membered metallacycles. In both cases, the NHC and phosphine moieties are situated in a *trans* position to the σ-aryl and ylide fragments, respectively (C1−Pd1−C13: [**4**](OTf) 173.88(10)°, [**14**](BF$_4$) 176.19(14); C7−Pd1−P1: [**4**](OTf) 170.88(7)°, [**14**](BF$_4$) 168.70(10)°). The four coordination bonds around metal atom fall in the classical range for these donor ligands (NHC: C1−Pd1 2.031(3) Å for [**4**](OTf), 2.014(4) Å for [**14**](BF$_4$); phosphine: P1−Pd1 2.2824(6) Å for [**4**](OTf), 2.2736(9) Å for [**14**](BF$_4$); ylide: C7−Pd1 2.118(2) Å for [**4**](OTf), 2.116(4) Å for [**14**](BF$_4$); phenyl: C13−Pd1 2.078(3) Å for [**4**](OTf), 2.050(3) Å for [**14**](BF$_4$)), in perfect agreement with their respective hybridization state.[16,17] Compared to related 6,6-*ortho*-metallated NHC core, bis(phosphonium ylide)- and NHC core, phosphonium ylide, phenolate Pd(II) complexes (173.95(18)° and 177.95(3)°),[16,17] 5,6-*ortho*-metallated Pd(II) complexes exhibit slightly narrower bite angles (C7−Pd1−P1: [**4**](OTf) 170.88(7)°, [**14**](BF$_4$) 168.70(10)°).

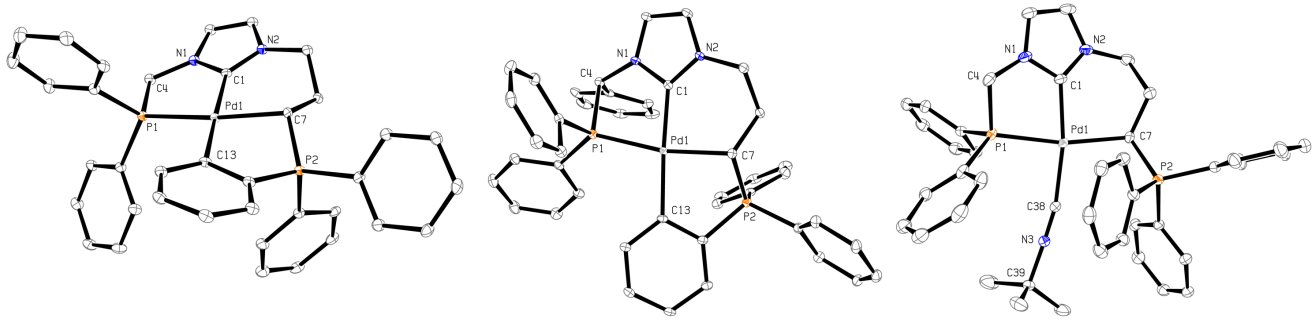

Figure 1. Perspective views of the cationic parts of Pd(II) *ortho*-metallated complexes [**4**](OTf) (left), R_{C4},R_{C7}-[**14**](BF$_4$) (middle, only one independent molecule shown) and pincer Pd(II) complex [**6**](OTf)$_2$ (right). Thermal ellipsoids set at the 20% probability level, hydrogen atoms, solvate molecules and counter anions are omitted for clarity.

Table 1. Selected Bond Lengths (Å) and Valent Angles (°) for Pd(II) Complexes [4](OTf), [6](OTf)$_2$ and [14](BF$_4$).

Complex	[**4**](OTf)	[**14**](BF$_4$)	[**6**](OTf)$_2$
Pd1−C1	2.031(3)	2.014(4)	1.991(3)
Pd1−C7	2.118(2)	2.116(4)	2.140(3)
Pd1−C13	2.078(3)	2.050(3)	–
Pd1−P1	2.2824(6)	2.2736(9)	2.2785(8)
C4−P1	1.874(3)	1.886(4)	1.836(4)
C7−P2	1.767(3)	1.767(4)	1.787(4)
C38−Pd1	–	–	2.014(3)
C38−N3	–	–	1.144(4)
C39−N3	–	–	1.468(4)
C1−Pd1−X (C13 or C38)	173.88(10)	176.19(14)	170.66(14)
C7−Pd1−P1	170.88(7)	168.70(10)	168.70(10)
C1−Pd1−C7	88.79(10)	89.18(14)	87.99(14)
C1−Pd1−P1	82.17(8)	80.16(10)	80.72(11)
C7−Pd1−C13	87.67(11)	88.07(14)	–
Pd1−C38−N3	–	–	169.1(3)
τ4	0.11	0.11	0.15

Complex [**6**](OTf)$_2$ represents the first example of Pd(II) derivative featuring 5,6-pincer ligand based on electron-rich chelating NHC-ylide scaffold. According to structural data the two fused palladacycles are strongly distorted with phosphine and ylide extremities being in a mutual *trans* arrangement (C7−Pd1−P1 168.70(10)°), and coordinated *t*-butylisonitrile in *trans* position to NHC core (C1−Pd1−C38 170.66(14)°). The Pd−C bond distances involving NHC, ylide and isonitrile (NHC: C1−Pd1 1.991(3) Å; ylide: C7−Pd1 2.140(3) Å; isonitrile: C38−Pd1 2.014(3) Å) are within the typical range of those reported in related Pd(II) complexes.[16,17,23] It's worth mentioning that the passage from *ortho*-metallated precursor [**4**](OTf) to the pincer form [**6**](OTf)$_2$ leads to concomitant shortening of Pd−NHC and lengthening of Pd−ylide bond distances, which can be due to different steric demands around the Pd center. For its part, Pd−P bond length remains quasi-unchanged between the two forms (2.2824(6) *vs.* 2.2785(8) Å). Noteworthy, the bite angle value (C7−Pd1−P1 168.70(10)°) is smaller than that of *dl*-isomer of the corresponding 6,6-*t*BuNC adduct of NHC core, bis(phosphonium ylide) ligand (170.1(3)°) but remains bigger than that of *meso*-isomer of the same ligand (165.42(11)°), an unexpected trend, which might be explained by a strong distortion observed in the *meso*-isomer.[16a] Finally, the non-linearity of the Pd−CN*t*Bu fragment can be tentatively rationalized by the bulkiness of proximal PPh_3^+ group (C1−Pd1−C38 170.66(14) Å and Pd1−C38−N3 169.1(3) Å). Such deviation was already observed in related pincer Pd(II) complexes exhibiting peripheral phosphonium ylide extremity.[16,17,23]

Theoretical Study of the Electronic Structure of Pd(II) Complex 15 Bearing Two types of Phosphonium Ylide Ligands by QTAIM and ELF Topological Analyses. Since all our efforts to grow single crystals of Pd(II) complex **15** suitable for X-ray diffraction were unsuccessful, we decided to investigate its structure by DFT methods. At the PBE-D3/6-31G**/LANL2DZ*(Pd) level of calculation, two minima for complex **15** were revealed on potential energy surface (Scheme 7) namely **15a**, featuring a non-conventional NHC-phosphonium ylide moiety suggested on the basis of experimental observations and **15b**, which can be described as a *C*-metalated form with a pending phosphine. It was found that **15a**, exhibiting a *P*-metalated ylide fragment was much more stable thermodynamically by +26.5 kcal.mol^{-1} relatively to the *C*-metalated isomer **15b**. This calculated relative Gibbs free energy is therefore in agreement with NMR data, suggesting the existence of a single complex featuring a PPh_2 donor group directly coordinated to the metal center. This unusual structure prompted us to use complementary theoretical tools such as Quantum Theory of Atoms in Molecules (QTAIM) and Electron Localization Function (ELF) topological analyses to investigate the nature of the *P*-metalated phosphonium ylide fragment in complex **15a**.

Scheme 7. Calculated Structures of Two Possible Isomers of Pd(II) Complex 15 at PBE-D3/6-31G/LANL2DZ*(Pd) Level of Calculation (Atoms Color Code: C − grey, N − blue, P – green, Pd − Dark Green.).**

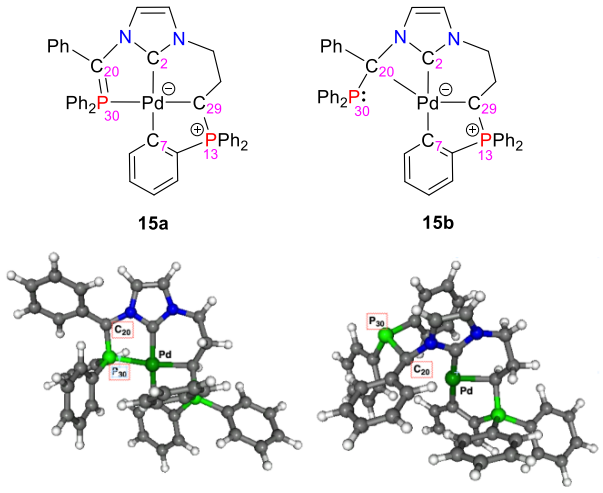

The QTAIM descriptors of all Pd−C bonds, except Pd−C20 bond, are very similar in both investigated isomers **15a** and **15b** (Figure 2, Table 2, Table S2 for QTAIM charges). According to the classification introduced by Bianchi et al.,[28] the values of $|V_{bcp}|/G_{bcp}$ of about 1.5 fall in the intermediate region between ionic ($|V_{bcp}|/G_{bcp} \leq 1$) and covalent bonding ($|V_{bcp}|/G_{bcp} \geq 2$), expected for dative bonding. The electron density and energy densities values are close to those already reported for similar metal-carbon bonds in Pd(II)[23] or Ni(II) pincer complexes.[14b,29] Based on the Espinosa-Molins-Lecomte correlation (E_{int}),[30] for both complexes, the strength of the Pd−C bond is stronger with NHC about 60 kcal.mol^{-1} than with ylide approaching 40 kcal.mol^{-1}. The large value of the delocalization index (DI = 0.8) suggests the presence of single Pd−C bond of significant covalence degree also highlighted by the $|H_{bcp}|/\rho_{bcp}$ ratio of 0.4. In isomer **15a**, the absence of any Bond Critical Point (BCP) related to the existence of a Pd−C20 bond is noticeable, while a Pd−P30 BCP, exhibiting QTAIM descriptors close to those of Pd−C dative bonds described above and to that expected for a dative Pd−P bond, is evidenced (Figure 2). In contrast, a Pd−C20 BCP related to an ionic interaction of C20 atom with the metal center is found in isomer **15b**, as indicated by the corresponding descriptors: $|V_{bcp}|/G_{bcp}$ = 1.03, low electron density (0.0287 a.u.) and Laplacian (0.070 a.u.) values at the BCP. The corresponding bond strength (E_{int} = 5.8 kcal.mol^{-1}) and DI index of 0.31 are also in favor of a weak

Table 2. Main QTAIM Descriptors (in a.u.) of the Bond Critical Points (BCPs) Related to Selected Bonds in 15a and 15b.

Complex	BCP	Bond	ρ_{bcp}	$\Delta\rho_{bcp}$	$\lvert {}^{a}\boldsymbol{H}_{bcp}\rvert/\rho_{bcp}$	$\lvert {}^{b}\boldsymbol{V}_{bcp}\rvert / \boldsymbol{G}_{bcp}$	DI[c]	E_{int}, kcal.mol^{-1}
15a								
	1	Pd−C2	0.1248	+0.289	0.41	1.42	0.84	55.1
	9	Pd−C7	0.1141	+0.220	0.40	1.46	0.83	46.1
	40	Pd−C29	0.0988	+0.180	0.38	1.46	0.72	37.7
	8	Pd−P30	0.0927	+0.114	0.40	1.56	0.78	32.0
	46	P30−C20	0.1689	+0.024	0.96	1.96	0.87	103.4
	19	P13−C29	0.1721	−0.147	1.00	2.27	0.82	96.7
15b								
	1	Pd−C2	0.1378	+0.328	0.44	1.42	0.86	63.3
	8	Pd−C7	0.1110	+0.231	0.39	1.43	0.81	45.3
	18	Pd−C29	0.1033	+0.163	0.40	1.50	0.80	38.6
	32	Pd−C20	0.0287	+0.070	0.0	1.03	0.31	5.8
	43	P30−C20	0.1501	−0.175	0.93	2.45	0.84	74.2
	22	P13−C29	0.1701	−0.164	1.00	2.32	0.80	93.9

[a] Energy density. [b] Potential energy density. [c] Delocalization index. PBE-D3/6-31G**/LANL2DZ*(Pd) level of calculation.

interaction between Pd and C20 atoms. As compared to the *C*-coordinated phosphonium ylide fragment (P13−C29), the QTAIM descriptors of P30−C20 bond are very similar in **15b** and slightly affected by the bonding of P-atom to Pd in form **15a**. The $\lvert \boldsymbol{V}_{bcp}\rvert/\boldsymbol{G}_{bcp}$ value of 2.45 in **15b** for P30−C20 bond, clearly related to strong covalent P−C bonding, decreases down to 1.96 in **15a** at the lower limit of covalent P−C bonding domain. The ELF description of both investigated isomers **15a** and **15b** are compared in Table 3. In both isomers, similarly to the above QTAIM descriptors, the ELF descriptors of the three following Pd−C bonds, C2−Pd, C7−Pd, and C29−Pd, are all very similar to those already reported for Ni−C bonds in pincer-type complexes.[14b,29] Furthermore, from ELF analysis, two distinct coordination modes of the P30−C20 moiety may be evidenced in **15a-b**. In **15a**, the presence of a monosynaptic basin V(C20) without any atomic contribution of Pd nor any sizeable covariance with the C(Pd) core basin, indicates that the P30−C20 fragment is coordinated to the Pd center by P30 only. The Pd−P30 bond is characterized by a disynaptic V(Pd, P30) valence basin with a population of 2.04 *e* and a large covariance in absolute value between this valence basin and the core basin of Pd ($<\sigma^2$(V(Pd, P30), C(Pd))$>$ = −0.39 (Table 3), in agreement with a dative bonding of significant covalent character already assigned to this bond from the above QTAIM descriptors. The population of the disynaptic valence basin V(P30, C20), close to 3 *e* and larger than that of the *C*-bonded ylide bond P13−C29 (2.73 *e* vs 2.18 *e,* respectively), thus suggests a more pronounced double bond character for P30−C20 bond interacting with the Pd atom by P30 only. The noticeable double bond character of the P30−C20 bond is also suggested by a slightly shorter bond length (1.77 Å) than that of the P13−C29 bond (1.79 Å). Both mesomeric forms involving a neutral ylene P=C **15a1** and a α-carbanionic phosphine **15a2** are thus representative with a similar weight for the chemical description of isomer **15a** (Scheme 8, up). In **15b**, the ELF description confirms the absence of bonding between the P30 atom of the PPh_2 donor group and the Pd center, already evidenced from the above QTAIM analysis. However, the presence of a monosynaptic basin V(C20) with a sizeable atomic contribution of Pd (5%) and significant covariance with the C(Pd) core basin ($<\sigma^2$(V(C20), C(Pd))$>$ = −0.12, Table 3) suggests the existence of a weak Pd−C20 interaction, as already evidenced by QTAIM analyses (Table 2). The ELF

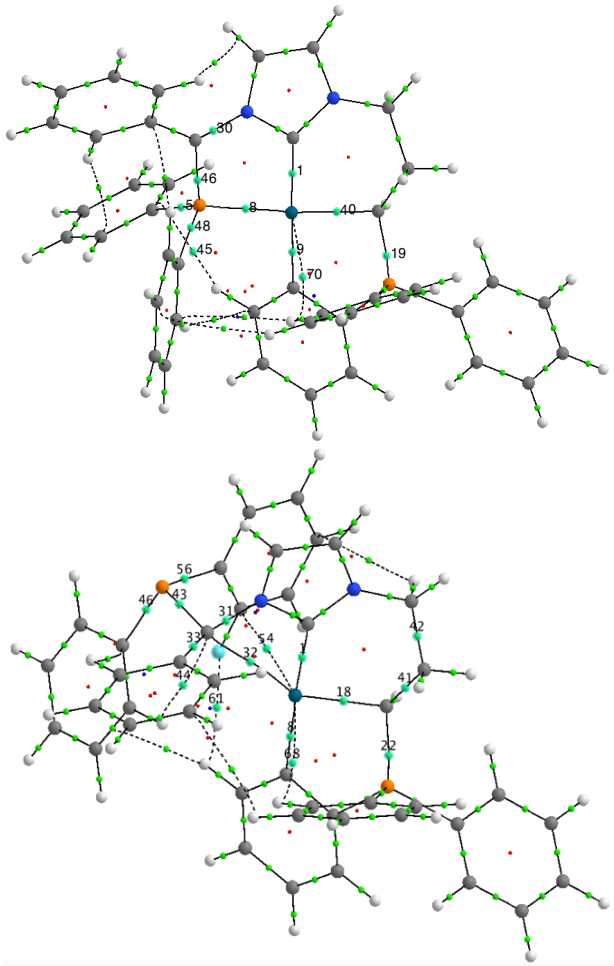

Figure 2. QTAIM molecular graphs of **15a** (top) and **15b** (bottom) calculated at the PBE-D3/6-31G**/LANL2DZ*(Pd) level. Selected bond critical points are located as small blue spheres.

Table 3. ELF Descriptors of Pd−C and Pd−P Interactions in Calculated Isomers 15a and 15b.

Complex	Valence basin	Ñ[a]	%Pd[b]	Cov.[c]
15a				
	V(Pd,C2)	2.64	0.26 (10 %)	−0.42
	V(Pd,C7)	2.20	0.25 (11%)	−0.40
	V(Pd,C29)	1.48	0.16 (11%)	−0.27
	V(Pd,P30)	2.04	0.30 (15%)	−0.39
	V(P13,C29)	2.18	0.0	−0.05
	V(P30,C20)	2.73	0.0	−0.02
	V(C20)	0.88	0.0	−0.0
15b				
	V(Pd,C2)	2.48	0.28 (11%)	−0.45
	V(Pd,C7)	2.26	0.24 (11%)	−0.40
	V(Pd,C29)	1.37	0.17 (12%)	−0.30
	V(P13,C29)	2.19	0.01	−0.07
	V(P30,C20)	1.92	0.0	−0.0
	V(C20)	1.42	0.07 (5%)	−0.12

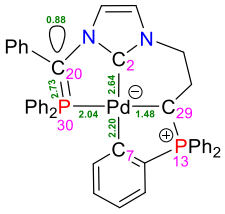

15a

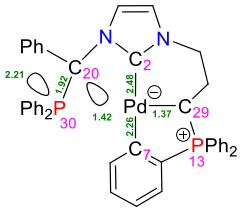

15b

[a] Average population Ñ of the ELF valence basin V (in *e*). [b] QTAIM atomic contribution of Pd to the valence basin V. [c] covariance $<\sigma^2(V(Pd, X), C(Pd))>$, X = C or P. PBE-D3/6-31G**/LANL2DZ*(Pd) level of calculation.

populations, atomic contributions of Pd and covariances with the C(Pd) core basin listed in Table 3 are thus consistent with two mesomeric forms of different weight for complex **15b** (Scheme 8, down). Given the absence of disynaptic valence

Scheme 8. Relative Weights of the Mesomeric Forms in Isomers 15a and 15b Suggested from the ELF Valence Basins Populations and Covariances Values.

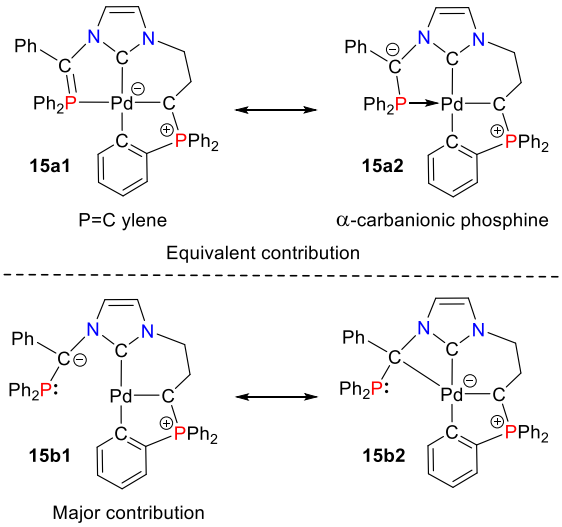

basin V(Pd, C20), the major form **15b1** corresponds to an unsaturated Pd(II) complex which may explain the much lower stability calculated for isomer **15b** as compared to **15a** (relative Gibbs free energy of +26.5 kcal.mol^{-1} at the PBE-D3/6-31G**/LANL2DZ*(Pd) level of calculation already mentioned above). Finally, it should be noted that P30−C20 (1.865 Å) and P13−C29 (1.801 Å) bond distances in the major isomer of **15b** are consistent with single P−C and ionic ylide P$^+$−C$^-$ bonds, respectively.

Both QTAIM and ELF analyses are fully consistent for the description of the most stable isomer **15a** featuring a NHC core pincer Pd complex containing as side extremities *C*-and *P*-pallada-substituted phosphonium ylides. The current situation contrasts with that observed in Mn(I) chemistry, where 18-e octahedral NHC-phosphinomethanide derivative *fac*-[(Ph_2PCHNHC)Mn($CO)_3$] was found to be more stable than its 16-e square-pyramidal *fac*-[(Ph_2P=CHNHC)Mn($CO)_3$] form exhibiting *P*-substituted phosphonium ylide with a difference of energy of 7.5 kcal.mol^{-1}.[26]

CONCLUSION

The extension of a synthetic strategy developed for the preparation of 6,6-NHC core, phosphonium ylide-based Pd(II) complexes to their nonsymmetrical 5,6-counterparts is here reported. Specifically, [*C,C,P*-Pd(L)]($OTf)_2$ (L = MeCN, *t*BuNC) pincer complexes were obtained from easily accessible phosphine-imidazolium precursor *via* a sequence of base-assisted activation of three C−H bonds and selective acidic cleavage of a C_{aryl}−Pd bond in corresponding *ortho*-metalated Pd(II) intermediate. On the basis of experimental IR ν_{CN} frequencies, electronic donation of this *P,C,C*-pincer ligand was found to compete with related *C,C,C*- and *C,C,O*-NHC core, phosphonium ylide-based ligands featuring a NHC or a phenolate as third extremity, respectively. The incorporation of a phenyl substituent at the phosphine side arm increasing the acidity of corresponding C−H bond in the *ortho*-metalated derivative allowed to prepare by basic treatment a unique Pd(II) complex perfectly stable in solution up to 0 °C, in which the metal center is coordinated by two different phosphonium ylides, one bounded in a conventional manner by its *C*-atom and the other in a nonconventional fashion by its *P*-atom. While DFT calculations confirmed that the form featuring non-conventional *P*-pallada-substituted ylide corresponds to the most thermodynamically stable isomer being strongly preferred relative to *C*-cyclometalated form, QTAIM and ELF topological analyses revealed that the nature of P−C ylide bond in such complex can be also rationalized by the existence of a mesomeric form of equivalent weight involving a α-carbanionic phosphine coordinated to Pd. The application of these NHC-ylide pincer complexes in homogeneous catalysis where high electronic density and non-innocent character would be simultaneously brought by two phosphonium ylides featuring different coordination mode is now an ambitious objective to be explored.

EXPERIMENTAL SECTION

General Remarks. All manipulations were conducted under an inert atmosphere of dry nitrogen or argon by using standard vacuum line and Schlenk tube techniques. Glassware was dried at 120 °C in an oven before use. Dry and oxygen-free solvents (CH_2Cl_2, Et_2O, THF, toluene, pentane) were obtained using a LabSolv solvent purification system. CH_3CN was dried using a MBraun SPS column. A liquid ethanol/nitrogen slush bath was used to keep samples at the selected low tempera-

ture. Compounds **1**[11f] [**11**](Br)[16a] and [**12**](BF$_4$)[24a] were synthetized according to known procedures. All other reagent-grade chemicals were purchased from commercial sources and used without additional purification. Chromatographic purification was carried out on silica gel (SiO_2, 63−200 µm). Solution IR spectra were recorded in 0.1 mm CaF_2 cells with a Perkin Elmer Frontier FT-IR spectrometer. ^{1}H, ^{13}C, and ^{31}P NMR spectra were obtained on Bruker AV300, AV400 or NEO600 spectrometers. NMR chemical shifts δ are given in ppm, with positive values to high frequency referenced against the residual signals of deuterated solvents for ^{1}H and ^{13}C and 85% H_3PO_4 for ^{31}P. Additional information on the carbon signal attribution was provided using ^{13}C{^{1}H, ^{31}P}, *J*-modulated spin−echo (JMOD) ^{13}C{^{1}H}, ^{1}H−^{13}C HMQC and HMBC experiments. MS spectra (ESI mode) were conducted by the mass spectrometry service of the Institut de Chimie de Toulouse-UAR 2599 using a Xevo G2 QTof (Waters) spectrometer. Elemental analyses were performed by the elemental analysis service of the LCC-UPR CNRS 8241 with a Perkin Elmer 2400 series II analyzer. No uncommon hazards are noted.

Synthesis of imidazolium salt [2]Br$_2$. Substituted imidazole **1** (1.10 g, 3.9 mmol) and (3-bromopropyl)triphenylphosphonium bromide (1.99 g, 4.3 mmol) were heated at 120 °C in DMF (25 mL) for 15 hours. After evaporation of the solvent under vacuum, [**2**]Br$_2$ was obtained as a white powder (2.76 g, 95%). Recrystallization from CH_2Cl_2/Et_2O at RT gave colorless crystals, some of them being suitable for X-ray diffraction analysis. ^{1}H NMR (400 MHz, $CDCl_3$, 25 °C): δ 10.21 (brs, 1H, N$_2$C*H*), 8.29 (brs, 1H, C*H*$_{Ph}$), 7.93−7.67 (m, 20H, C*H*$_{Ph}$), 7.47−7.42 (m, 6H, C*H*$_{Ph}$), 5.44 (d, $^2J_{HP}$ = 6.0 Hz, 2H, P(O)C*H*$_2$), 4.80 (t, $^3J_{HH}$ = 6.8 Hz, 2H, NC*H*$_2$), 3.85−3.78 (m, 2H, PC*H*$_2$), 2.32−2.26 (m, 2H, CH$_2$). ^{31}P{^{1}H} NMR (162 MHz, $CDCl_3$, 25 °C): δ 26.1 (s), 24.4 (s). ^{13}C NMR (101 MHz, $CDCl_3$, 25 °C): δ 137.1 (s, N$_2$*C*H), 135.2 (d, J_{CP} = 3.1 Hz, *C*H$_{Ph}$), 133.9 (d, J_{CP} = 10.2 Hz, *C*H$_{Ph}$), 133.0 (d, J_{CP} = 2.7 Hz, *C*H$_{Ph}$), 131.3 (d, J_{CP} = 9.9 Hz, *C*H$_{Ph}$), 130.6 (d, J_{CP} = 12.7 Hz, *C*H$_{Ph}$), 129.2 (d, J_{CP} = 12.4 Hz, *C*H$_{Ph}$), 127.9 (d, $^1J_{CP}$ = 103.3 Hz, *C*$_{Ph}$), 123.7, 122.6 (s, CH$_{Im}$), 117.4 (d, $^1J_{CP}$ = 86.7 Hz, C$_{Ph}$), 49.0 (d, $^1J_{CP}$ = 90.9 Hz, P(O)*C*H$_2$), 48.8 (s, N*C*H$_2$), 24.2 (d, $^2J_{CP}$ = 2.7 Hz, *C*H$_2$), 19.8 (d, $^1J_{CP}$ = 53.8 Hz, P*C*H$_2$); MS (ES$^+$): *m/z*: 665.1 [M − Br]$^+$; HRMS (ES$^+$): calcd for $C_{37}H_{36}BrN_2OP_2$, 665.1486; found, 665.1468 (ε_r = 2.7 ppm). Mp 63−65°C.

Synthesis of pre-ligand [3](OTf)$_2$. [**2**]Br$_2$ (2.10 g, 2.8 mmol), $PhSiH_3$ (1.35 mL, 11.0 mmol) in the presence of bis-4-nitrophenyl phosphate (0.10 g, 0.28 mmol) were heated at 120 °C in degassed C_6H_5Cl (30 mL) for 16 hours. After evaporation of the solvent under vacuum, the crude residue and NaOTf (1.30 g, 7.5 mmol) were stirred in CH_2Cl_2 (30 mL) at RT for 12 hours. After filtration over Celite and evaporation of the solvent, the solid residue was washed several times with Et_2O (3×10 mL) affording [**3**](OTf)$_2$ as a white powder (2.30 g, 96%). ^{1}H NMR (400 MHz, $CDCl_3$, 25 °C): δ 8.96 (brs, 1H, N$_2$C*H*), 7.80−7.62 (m, 17H, C*H*$_{Ph}$), 7.42−7.32 (m, 9H, C*H*$_{Ph+Im}$), 6.99 (brs, 1H, C*H*$_{Im}$), 4.85 (d, $^2J_{HP}$ = 5.9 Hz, 2H, P(O)C*H*$_2$), 4.49−4.45 (m, 2H, NC*H*$_2$), 3.39−3.32 (m, 2H, PC*H*$_2$), 2.19−2.14 (m, 2H, C*H*$_2$). ^{31}P{^{1}H} NMR (162 MHz, $CDCl_3$, 25 °C): δ 24.0 (s, $^+$PPh$_3$), −12.6 (s, PPh$_2$). ^{13}C{^{1}H} NMR (101 MHz, $CDCl_3$, 25 °C): δ 136.3 (s, N$_2$*C*H), 135.4 (d, J_{CP} = 3.0 Hz, *C*H$_{Ph}$), 133.7 (d, J_{CP} = 10.1 Hz, *C*H$_{Ph}$), 133.0 (d, J_{CP} = 20.1 Hz, *C*H$_{Ph}$), 132.6 (d, J_{CP} = 12.1 Hz, *C*$_{Ph}$), 130.7 (d, J_{CP} = 13.1 Hz, *C*H$_{Ph}$), 130.4 (s, *C*H$_{Ph}$), 129.4 (d, J_{CP} = 7.0 Hz, *C*H$_{Ph}$), 123.7 (s, *C*H$_{Im}$), 122.1 (s, *C*H$_{Im}$), 120.6 (q, $^1J_{CF}$ = 322.0 Hz, *C*F$_3$), 117.4 (d, $^1J_{CP}$ = 87.5 Hz, *C*$_{Ph}$), 49.5 (d, J_{CP} = 23.1 Hz, *C*H$_2$), 49.0 (d, J_{CP} = 23.1 Hz, *C*H$_2$), 24.4 (s, *C*H$_2$), 19.7 (d, J_{CP} = 54.3 Hz, P*C*H$_2$); MS (ES$^+$): *m/z*: 719.2 [M − CF_3SO_3]$^+$. HRMS (ES$^+$): calcd for $C_{38}H_{36}F_3N_2O_3P_2S$, 719.1874; found, 719.1882 (ε_r = 1.1 ppm). Mp 38−40°C.

Synthesis of complex [4](OTf). A mixture of [**3**](OTf)$_2$ (0.34 g, 0.39 mmol), $PdCl_2$ (0.07 g, 0.39 mmol), and anhydrous Cs_2CO_3 (0.89 g, 2.74 mmol) was stirred at 50 °C in MeCN (20 mL) for 12 hours. After filtration over Celite and evaporation of the solvent under vacuum, the crude residue was dissolved in CH_2Cl_2 (10 mL), and the solution was filtered over Celite. Purification by chromatography on silica gel (CH_2Cl_2/MeOH 99/1) gave [**4**](OTf) as a white powder (0.24 g, 74%). Recrystallization from CH_2Cl_2/Et_2O at RT gave pale yellow crystals, some of them being suitable for X-ray diffraction analysis. ^{1}H NMR (400 MHz, CD_3CN, 25 °C): δ 7.86−7.78 (m, 5H, C*H*$_{Ph}$), 7.74−7.68 (m, 4H, C*H*$_{Ph}$), 7.64−7.52 (m, 9H, C*H*$_{Ph}$), 7.48−7.43 (m, 3H, C*H*$_{Ph}$), 7.24 (d, J_{HH} = 4.0 Hz, 1H, C*H*$_{Im}$), 7.17 (t, J_{HH} = 4.0 Hz, 1H, C*H*$_{Im}$), 7.14−7.03 (m, 3H, C*H*$_{Ph}$), 4.89 (dd, $^2J_{HH}$ = 14.5 Hz, $^2J_{HP}$ = 9.2 Hz, 1H, PC*H*$_2$), 4.68 (dd, $^2J_{HH}$ = 14.5 Hz, $^2J_{HP}$ = 4.1 Hz, 1H, PC*H*$_2$), 4.36−4.30 (m, 1H, NC*H*$_2$), 4.18−4.11 (m, 1H, NC*H*$_2$), 3.33−3.24 (m, 1H, PC*H*), 2.58−2.48 (m, 1H, C*H*$_2$), 1.90−1.82 (m, 1H, C*H*$_2$). ^{31}P{^{1}H} NMR (162 MHz, CD_3CN, 25 °C): δ 43.3 (d, $^3J_{PP}$ = 16.5 Hz, PPh$_2$), 34.4 (d, $^3J_{PP}$ = 16.5 Hz, $^+$PPh$_3$). ^{13}C{^{1}H} NMR (101 MHz, CD_3CN, 25 °C): δ 178.8 (dd, J_{CP} = 12.1, 6.3 Hz, Pd−*C*N$_2$), 175.8 (dd, $^2J_{CP}$ = 35.2, 6.2 Hz, Pd−*C*$_{Ph}$), 142.6 (dd, J_{CP} = 19.1, 11.6 Hz, *C*H$_{Ph}$), 139.3 (d, $^1J_{CP}$ = 117.6 Hz, *C*$_{Ph}$) 135.1 (d, J_{CP} = 8.7 Hz, *C*H$_{Ph}$), 134.5 (d, J_{CP} = 14.1 Hz, *C*H$_{Ph}$), 134.4 (d, J_{CP} = 14.1 Hz, *C*H$_{Ph}$), 134.3 (d, J_{CP} = 2.9 Hz, *C*H$_{Ph}$), 133.9 (d, J_{CP} = 9.5 Hz, *C*H$_{Ph}$), 133.8 (d, J_{CP} = 3.0 Hz, *C*H$_{Ph}$), 132.8 (d, J_{CP} = 2.4 Hz, *C*H$_{Ph}$), 132.7 (d, J_{CP} = 2.3 Hz, *C*H$_{Ph}$), 131.6 (d, J_{CP} = 19.7 Hz, *C*H$_{Ph}$), 131.4 (t, J_{CP} = 3.4 Hz, *C*H$_{Ph}$), 131.0 (d, $^1J_{CP}$ = 36.4 Hz, *C*$_{Ph}$), 130.7 (d, J_{CP} = 10.5 Hz, *C*H$_{Ph}$), 130.4 (d, J_{CP} = 10.3 Hz, *C*H$_{Ph}$), 130.2 (d, J_{CP} = 10.4 Hz, *C*H$_{Ph}$), 129.9 (d, J_{CP} = 11.6 Hz, *C*H$_{Ph}$), 126.7 (d, $^1J_{CP}$ = 58.6 Hz, *C*$_{Ph}$), 126.5 (d, $^1J_{CP}$ = 57.6 Hz, *C*$_{Ph}$), 126.1 (d, J_{CP} = 13.2 Hz, *C*H$_{Ph}$), 124.1 (s, *C*H$_{Im}$), 120.6 (d, $^3J_{CP}$ = 8.4 Hz, *C*H$_{Im}$), 120.5 (q, $^1J_{CF}$ = 320.1 Hz, *C*F$_3$), 54.2 (d, $^1J_{CP}$ = 35.2 Hz, P*C*H$_2$), 53.6 (d, $^3J_{CP}$ = 22.2 Hz, N*C*H$_2$), 26.7 (d, $^2J_{CP}$ = 3.8 Hz, *C*H$_2$), 25.4 (dd, $^1J_{CP}$ = 85.1 Hz, $^2J_{CP}$ = 41.3 Hz, P*C*H). MS (ES$^+$): *m/z*: 673.1 [M − (CF_3SO_3)]$^+$. HRMS (ES$^+$): calcd for $C_{37}H_{33}N_2P_2Pd$, 673.1154; found, 673.1199 (ε_r = 6.7 ppm). Mp 210−212°C.

Synthesis of complex [5](OTf)$_2$. TfOH (0.5 M in MeCN, 293 µL, 0.15 mmol) was added at −40 °C to a solution of [**4**](OTf) (0.13 g, 0.15 mmol) in MeCN (5 mL). The mixture was warmed to RT for 2 hours. After filtration over Celite, the solvent was removed under vacuum, and complex [**5**](OTf)$_2$ was obtained as a pale yellow powder (0.16 g, 97%). ^{1}H NMR (400 MHz, CD_3CN, 25 °C): δ 7.86−7.81 (m, 6H, C*H*$_{Ph}$), 7.79−7.75 (m, 3H, C*H*$_{Ph}$), 7.70−7.55 (m, 14H, C*H*$_{Ph}$), 7.52−7.47 (m, 2H, C*H*$_{Ph}$), 7.44 (d, J_{HH} = 4.0 Hz, 1H, C*H*$_{Im}$), 7.14 (d, J_{HH} = 4.0 Hz, 1H, C*H*$_{Im}$), 4.99 (dd, $^2J_{HH}$ = 14.9 Hz, $^2J_{HP}$ = 9.8 Hz, 1H, PC*H*$_2$), 4.88 (dd, $^2J_{HH}$ = 14.9 Hz, $^2J_{HP}$ = 4.6 Hz, 1H, PC*H*$_2$), 4.11−4.04 (m, 1H, NC*H*$_2$), 3.93−3.86 (m, 1H, NC*H*$_2$), 3.61−3.52 (m, 1H, PC*H*), 2.37−2.26 (m, 2H, C*H*$_2$). ^{31}P{^{1}H} NMR (162 MHz, CD_3CN, 25 °C): δ 42.4 (d, $^3J_{PP}$ = 2.4 Hz, PPh$_2$), 31.0 (d, $^3J_{PP}$ = 2.4 Hz, $^+$PPh$_3$). ^{13}C{^{1}H} NMR (101 MHz, CD_3CN, 25 °C): δ 156.8 (d, J_{CP} = 7.0 Hz, Pd−*C*N$_2$), 135.0 (d, J_{CP} = 3.0 Hz, *C*H$_{Ph}$), 134.8 (d, J_{CP} = 9.0 Hz, *C*H$_{Ph}$), 134.4 (d, J_{CP} = 13.1 Hz, *C*H$_{Ph}$), 133.8 (d, J_{CP} = 12.1 Hz, *C*H$_{Ph}$), 133.8 (d, J_{CP} = 2.0 Hz, *C*H$_{Ph}$), 133.5 (d, J_{CP} = 2.0 Hz, *C*H$_{Ph}$), 130.7 (d, J_{CP} = 12.1 Hz, *C*H$_{Ph}$), 130.6 (d, J_{CP} = 11.1 Hz, *C*H$_{Ph}$), 127.2 (d, $^1J_{CP}$ = 44.2 Hz, *C*$_{Ph}$), 127.1 (d, $^1J_{CP}$ = 46.3 Hz, *C*$_{Ph}$), 124.9 (s, *C*H$_{Im}$), 123.8 (dd, $^1J_{CP}$ = 83.5 Hz, J_{CP} = 3.0 Hz, *C*$_{Ph}$), 122.9 (d, $^3J_{CP}$ = 11.1 Hz, *C*H$_{Im}$), 120.5 (q, $^1J_{CF}$ = 320.1 Hz, *C*F$_3$), 52.1 (d, $^3J_{CP}$ = 13.1 Hz, N*C*H$_2$), 49.6 (d, $^1J_{CP}$ = 38.2 Hz, P*C*H$_2$), 27.7 (dd, J_{CP} = 5.0, 3.0 Hz, *C*H$_2$), 14.6 (dd, $^1J_{CP}$ = 95.6 Hz, $^2J_{CP}$ = 30.1 Hz, P*C*H). MS (ES$^+$): *m/z*: 823.1 [M − (CF_3SO_3 + MeCN)]$^+$; HRMS (ES$^+$): calcd for $C_{38}H_{34}F_3N_2O_3P_2PdS$, 823.0752; found, 823.0762 (ε_r = 1.2 ppm). Mp 95−97°C.

Synthesis of complex [6](OTf)$_2$. *t*-Butylisocyanide (8.4 µL, 0.074 mmol) was added at −80 °C to a solution of [**5**](OTf)$_2$ (0.05 g, 0.049 mmol) in CH_2Cl_2 (5 mL). The mixture was warmed to RT for 2 hours. After filtration over Celite, the solvent was removed under vacuum, and complex [**6**](OTf)$_2$ was obtained as a pale yellow powder (0.05 g, 96%). Recrystallization from THF at −20 °C gave pale yellow crystals, some of them being suitable for X-ray diffraction analysis. ^{1}H NMR (400 MHz, CD_2Cl_2, 25 °C): δ 7.91−7.86 (m, 6H, C*H*$_{Ph}$), 7.81−7.75 (m, 5H, C*H*$_{Ph}$), 7.71−7.64 (m, 8H, C*H*$_{Ph}$), 7.62−7.54 (m, 7H, C*H*$_{Ph}$+C*H*$_{Im}$), 7.17 (brs, 1H, C*H*$_{Im}$), 5.18 (dd, $^3J_{HH}$ = 14.6 Hz, $^2J_{HP}$ = 7.3 Hz, 1H, PC*H*$_2$), 5.07 (dd, $^2J_{HH}$ = 14.6 Hz, $^2J_{HP}$ = 7.8 Hz, 1H, PC*H*$_2$), 4.30−4.20 (m, 2H, NC*H*$_2$), 3.37−3.27 (m, 1H, PC*H*), 2.34−2.27 (m, 1H, C*H*$_2$), 2.12−1.99 (m, 1H, C*H*$_2$), 0.42 (s, 9H, *t*Bu). ^{31}P{^{1}H} NMR (162 MHz, CD_2Cl_2, 25 °C): δ 45.5 (s, PPh$_2$), 34.2 (s, $^+$PPh$_3$). ^{13}C{^{1}H} NMR (101 MHz, CD_2Cl_2, 25 °C): δ 163.5 (d, J_{CP} = 7.1 Hz, Pd−*C*N$_2$), 134.6 (d, J_{CP} = 3.0 Hz, *C*H$_{Ph}$), 134.2 (d, J_{CP} = 9.1 Hz, *C*H$_{Ph}$), 134.0 (d, J_{CP} = 13.2 Hz, *C*H$_{Ph}$), 133.6 (s, *C*H$_{Ph}$), 133.5 (d, J_{CP} = 10.1 Hz, *C*H$_{Ph}$), 133.5 (s, *C*H$_{Ph}$), 132.0 (brs, *t*BuN*C*), 130.4 (d, J_{CP} = 10.1 Hz, *C*H$_{Ph}$), 130.3 (d, J_{CP} = 11.2 Hz, *C*H$_{Ph}$), 130.3 (s, *C*H$_{Ph}$), 125.7 (d, $^1J_{CP}$ = 48.8 Hz, *C*$_{Ph}$), 125.6 (d, $^1J_{CP}$ = 48.8 Hz, *C*$_{Ph}$), 124.2 (s, *C*H$_{Im}$), 123.7 (dd, $^1J_{CP}$ = 84.0 Hz, J_{CP} = 2.0 Hz, *C*$_{Ph}$), 122.1 (d, $^3J_{CP}$ = 11.2 Hz, *C*H$_{Im}$), 121.0 (q, $^1J_{CF}$ = 320.2 Hz, CF$_3$), 59.5 (s, *C*(CH$_3$)$_3$), 52.4 (d, $^3J_{CP}$ = 20.3 Hz, N*C*H$_2$), 51.1 (d, $^1J_{CP}$ = 37.5 Hz, P*C*H$_2$), 28.8 (s, C(*C*H$_3$)$_3$)), 27.8 (d, $^2J_{CP}$ = 3.0 Hz, *C*H$_2$), 11.9

(dd, $^1J_{CP}$ = 91.4 Hz, $^2J_{CP}$ = 34.5 Hz, PC*H*); MS (ES$^+$): *m/z*: 906.1 [M − (CF_3SO_3)]$^+$. IR (CH_2Cl_2): ν_{CN} 2206 cm^{-1} (s). HRMS (ES$^+$): calcd for $C_{43}H_{43}F_3N_3O_3P_2PdS$, 906.1487; found, 906.1501 (ε_r = 1.5 ppm). Mp 160−162°C.

Synthesis of phosphonium salt [11](BF$_4$). [**11**]Br (1.0 g, 2.2 mmol) and $NaBF_4$ (0.36 g, 3.3 mmol) were stirred in MeCN (30 mL) at RT for 12 hours. After evaporation of the solvent, the solid residue was extracted with CH_2Cl_2 (3×20 mL) and dried over Na_2SO_4. After filtration, the solvent was evaporated under vacuum, and the solid was washed with Et_2O (3×10 mL) and dried affording [**11**](BF$_4$) as a white powder (0.70 g, 70%). ^{1}H NMR (400 MHz, CD_3CN, 25 °C): δ 7.90–7.85 (m, 3H, C*H*$_{Ph}$), 7.74–7.62 (m, 12H, C*H*$_{Ph}$), 7.50 (brs, 1H, C*H*$_{Ph}$), 7.01 (brs, 1H, C*H*$_{Im}$), 6.95 (brs, 1H, C*H*$_{Im}$), 4.12 (t, $^3J_{HH}$ = 8.0 Hz, 2H, NCH_2), 3.16–3.08 (m, 2H, PCH_2), 2.10–2.00 (m, 2H, CH_2); ^{31}P{^{1}H} NMR (162 MHz, CD_3CN, 25 °C): δ 23.7 (s). ^{13}C{^{1}H} NMR (101 MHz, CD_3CN, 25 °C): δ 138.5 (brs, N_2CH), 136.3 (d, J_{CP} = 3.0 Hz, *C*H$_{Ph}$), 134.6 (d, J_{CP} = 10.1 Hz, *C*H$_{Ph}$), 131.3 (d, J_{CP} = 12.1 Hz, *C*H$_{Ph}$), 130.2 (s, *C*H$_{Im}$), 120.1 (s, *C*H$_{Im}$), 118.8 (d, $^1J_{CP}$ = 86.9 Hz, *C*$_{Ph}$), 47.0 (d, $^3J_{CP}$ = 19.2 Hz, NCH_2), 25.0 (d, $^2J_{CP}$ = 4.0 Hz, CH_2), 20.1 (d, $^1J_{CP}$ = 54.5 Hz, PCH_2). MS (ES$^+$): *m/z*: 371.2 [M – BF$_4$]$^+$. Mp 145−147°C. Anal. Found, C 61.57, H 4.79, N 5.93. Calcd. for $C_{24}H_{24}BF_4N_2P.0.15(CH_2Cl_2)$: C 61.59, H 5.20, N 5.95.

Synthesis of pre-ligand [13](BF$_4$)$_2$. Solid [**11**](BF$_4$) (1.32 g, 2.88 mmol) was added to a solution of [**12**]BF_4×0.25 CH_2Cl_2 (1.61 g, 2.88 mmol) in CH_2Cl_2 (20 mL) at RT. The color of the solution immediately changed from orange to yellow. After stirring at this temperature for 5 min, the resulting solution was transferred into a photochemical reactor, diluted with CH_2Cl_2 (*ca*. 200 mL), and HBF_4×OEt_2 was added (0.40 mL, 2.88 mmol). The solution was irradiated at RT with visible light under vigorous stirring until CO evolution ceased (~1h). The resulting suspension was then filtered over Celite and toluene (60 mL) was added. The solution was concentrated to a volume of 50 mL which induced precipitation of the product as a viscous oil. The supernatant was removed by decantation and the residue was washed with toluene (20 mL) and dried under vacuum to give [**13**](BF$_4$)$_2$ as a yellow powder (1.90 g, 80%). ^{1}H NMR (400 MHz, $CDCl_3$, 25 °C): δ 8.64 (s, 1H, N_2CH), 7.80–7.58 (m, 17H, C*H*$_{Ph}$), 7.41 (t, J_{HH} = 8.0 Hz, 2H, *C*H$_{Ph}$), 7.33–6.98 (m, 12H, C*H*$_{Ph+Im}$), 7.00 (t, J_{HH} = 8.0 Hz, 1H, C*H*$_{Ph}$), 6.20 (d, $^2J_{PH}$ = 4.0 Hz, 1H, C*H*$_{Ph}$), 4.34–4.28 (m, 1H, NCH_2), 4.23–4.17 (m, 1H, NCH_2), 3.18–3.10 (m, 2H, PCH_2), 2.11–2.02 (m, 2H, CH_2). ^{31}P{^{1}H} NMR (162 MHz, $CDCl_3$, 25 °C): δ 21.7 (s, $^+$PPh$_3$), −8.4 (s, PPh$_2$). ^{13}C{^{1}H} NMR (101 MHz, $CDCl_3$, 25 °C): δ 135.5 (d, J_{CP} = 3.0 Hz, *C*H$_{Ph}$), 135.4 (brs, N_2CH), 134.5 (d, J_{CP} = 14.1 Hz, *C*$_{Ph}$), 133.9 (d, J_{CP} = 22.2 Hz, *C*H$_{Ph}$), 133.6 (d, J_{CP} = 10.1 Hz, *C*H$_{Ph}$), 133.2 (d, J_{CP} = 19.2 Hz, *C*H$_{Ph}$), 133.1 (d, J_{CP} = 14.1 Hz, *C*$_{Ph}$), 131.9 (d, J_{CP} = 10.1 Hz, *C*$_{Ph}$), 130.8 (d, J_{CP} = 13.1 Hz, *C*H$_{Ph}$), 130.6 (s, *C*H$_{Ph}$), 130.0 (s, *C*H$_{Ph}$), 129.9 (s, *C*H$_{Ph}$), 129.7 (s, *C*H$_{Ph}$), 129.4 (d, J_{CP} = 10.1 Hz, *C*H$_{Ph}$), 129.3 (d, J_{CP} = 8.1 Hz, *C*H$_{Ph}$), 128.9 (d, J_{CP} = 7.1 Hz, *C*H$_{Ph}$), 124.1 (s, *C*H$_{Im}$), 120.2 (d, $^3J_{CP}$ = 6.1 Hz, *C*H$_{Im}$), 117.4 (d, $^1J_{CP}$ = 86.9 Hz, *C*$_{Ph}$), 64.3 (d, $^1J_{CP}$ = 16.2 Hz, *C*HPh), 49.0 (d, $^3J_{CP}$ = 23.2 Hz, NCH_2), 24.2 (s, CH_2), 20.0 (d, $^1J_{CP}$ = 55.5 Hz, PCH_2). MS (ES$^+$): *m/z*: 733.3 [M – BF$_4$]$^+$; HRMS (ES$^+$): calcd for $C_{43}H_{40}BN_2F_4P_2$, 733.2696; found, 733.2709 (ε_r = 1.8 ppm). Mp 80−82°C.

Synthesis of complex [14](BF$_4$). A mixture of [**13**](BF$_4$)$_2$ (0.34 g, 0.41 mmol), $PdCl_2$ (0.07 g, 0.41 mmol), and anhydrous Cs_2CO_3 (0.95 g, 2.90 mmol) was stirred at 50 °C in MeCN (30 mL) for 12 hours. After filtration over Celite and evaporation of the solvent under vacuum, the crude residue was dissolved in CH_2Cl_2 (10 mL), and the solution was filtered over Celite. After purification by chromatography on silica (CH_2Cl_2/MeOH 99/1) and recrystallization from CH_2Cl_2/Et_2O at RT, [**14**](BF$_4$) was obtained as a white powder (0.24 g, 69%) and as a mixture of two diastereomers (70/30). Single crystals of [**14**](BF$_4$) were obtained by vapor diffusion in a CH_2Cl_2/Et_2O mixture at RT. NMR assignment: [a]major isomer (70%); [b]minor isomer (30%). ^{1}H NMR (400 MHz, CD_3CN, 25 °C): δ 7.97–7.92^{a,b} (m, 2H, C*H*$_{Ph}$), 7.89–7.69^{a,b} (m, 12H, C*H*$_{Ph}$), 7.63–7.54^{a,b} (m, 6H, C*H*$_{Ph}$), 7.48–7.40^{a,b} (m, 2.6H, C*H*$_{Ph}$), 7.38–7.29^{a,b} (m, 4H, C*H*$_{Ph}$), 7.25–6.99^{a,b} (m, 12H, C*H*$_{Ph}$), 6.95–6.86^{a,b} (m, 2H, C*H*$_{Ph}$), 6.75–6.65^b (m, 0.8H, C*H*$_{Ph}$), 6.55^a (d, J_{HH} = 8.0 Hz, 2H, C*H*$_{Ph}$), 6.35^a (d, $^2J_{PH}$ = 8.0 Hz, 1H, C*H*Ph), 6.26^b (d, $^2J_{PH}$ = 8.0 Hz, 0.4H, C*H*Ph), 4.41–4.24^{a,b} (m, 1.8H, NCH_2), 4.20–4.13^a (m, 1H, NCH_2), 3.45–3.29^{a,b} (m, 1.4H, PC*H*), 2.70–2.50^{a,b} (m, 1.4H, CH_2), 2.10–2.00^{a,b} (m, 1.4H, CH_2). ^{31}P{^{1}H} NMR (162 MHz, CD_3CN, 25 °C): δ 61.3^b (d, $^3J_{PP}$ = 16.2 Hz, PPh$_2$), 60.3^a (d, $^3J_{PP}$ = 17.8 Hz, PPh$_2$), 34.9^b (d, $^3J_{PP}$ = 16.2 Hz, $^+$PPh$_3$), 32.1^a (d, $^3J_{PP}$ = 17.8 Hz, $^+$PPh$_3$). ^{13}C{^{1}H} NMR (101 MHz, CD_3CN, 25 °C): δ 179.4^a (dd, J_{CP} = 13.1, 6.1 Hz, Pd−*C*N$_2$), 178.6^b (dd, J_{CP} = 12.1, 7.1 Hz, Pd−*C*N$_2$), 176.4^a (dd, $^2J_{CP}$ = 34.3, 6.1 Hz, Pd−*C*$_{Ph}$), 175.3^b (dd, $^2J_{CP}$ = 35.3, 6.1 Hz, Pd−*C*$_{Ph}$), 143.3^a (dd, J_{CP} = 19.2, 12.1 Hz, *C*H$_{Ph}$), 141.9^b (dd, J_{CP} = 19.2, 11.1 Hz, *C*H$_{Ph}$), 139.3^b (d, $^1J_{CP}$ = 117.2 Hz, *C*$_{Ph}$), 139.1^a (d, $^1J_{CP}$ = 118.2 Hz, *C*$_{Ph}$), 136.7^b (d, J_{CP} = 15.1 Hz, *C*H$_{Ph}$), 136.6^a (d, J_{CP} = 3.0 Hz, *C*$_{Ph}$), 136.3^b (d, J_{CP} = 3.0 Hz, *C*$_{Ph}$), 136.0^a (d, J_{CP} = 13.1 Hz, *C*H$_{Ph}$), 135.1^a (d, J_{CP} = 9.1 Hz, *C*H$_{Ph}$), 134.9^b (d, J_{CP} = 8.1 Hz, *C*H$_{Ph}$), 134.4^a (d, J_{CP} = 2.0 Hz, *C*H$_{Ph}$), 134.0^a (d, J_{CP} = 10.1 Hz, C*H*$_{Ph}$), 133.8^a (d, J_{CP} = 3.0 Hz, *C*H$_{Ph}$), 133.7^b (d, J_{CP} = 12.1 Hz, *C*H$_{Ph}$), 133.7^b (d, J_{CP} = 3.0 Hz, *C*H$_{Ph}$), 132.8^b (d, J_{CP} = 3.0 Hz, *C*H$_{Ph}$), 132.7^a (d, J_{CP} = 2.0 Hz, *C*H$_{Ph}$), 132.6^a (d, J_{CP} = 2.0 Hz, *C*H$_{Ph}$), 132.3^b (d, J_{CP} = 3.0 Hz, *C*H$_{Ph}$), 131.6^a (d, J_{CP} = 20.2 Hz, *C*H$_{Ph}$), 131.5^b (d, J_{CP} = 19.2 Hz, *C*H$_{Ph}$), 131.3^a (brs, *C*H$_{Ph}$), 131.1^a (d, $^1J_{CP}$ = 29.3 Hz, *C*$_{Ph}$), 130.8^a (d, J_{CP} = 10.1 Hz, *C*H$_{Ph}$), 130.5^a (d, J_{CP} = 9.1 Hz, *C*H$_{Ph}$), 130.3^b (d, J_{CP} = 9.1 Hz, *C*H$_{Ph}$), 130.1^a (d, J_{CP} = 11.1 Hz, *C*H$_{Ph}$), 129.8^b (d, J_{CP} = 11.1 Hz, *C*H$_{Ph}$), 129.5^b (d, J_{CP} = 2.0 Hz, *C*H$_{Ph}$), 129.4^b (d, J_{CP} = 15.1 Hz, *C*H$_{Ph}$), 129.4^b (d, J_{CP} = 2.0 Hz, *C*H$_{Ph}$), 129.3^a (s, *C*H$_{Ph}$), 129.2^a (d, J_{CP} = 6.1 Hz, *C*H$_{Ph}$), 129.1^a (d, J_{CP} = 3.0 Hz, *C*H$_{Ph}$), 128.4^b (brs, *C*H$_{Ph}$), 127.7^a (d, J_{CP} = 5.0 Hz, *C*H$_{Ph}$), 127.2^b (d, $^1J_{CP}$ = 35.3 Hz, *C*$_{Ph}$), 127.0^a (d, $^1J_{CP}$ = 89.9 Hz, *C*$_{Ph}$), 126.8^a (d, $^1J_{CP}$ = 37.4 Hz, *C*$_{Ph}$), 126.5^a (d, $^1J_{CP}$ = 64.6 Hz, *C*$_{Ph}$), 126.5^a (d, $^1J_{CP}$ = 50.5 Hz, *C*$_{Ph}$), 126.5^b (d, $^1J_{CP}$ = 81.8 Hz, *C*$_{Ph}$), 126.1^b (d, J_{CP} = 16.2 Hz, *C*H$_{Ph}$), 126.0^a (d, J_{CP} = 13.1 Hz, *C*H$_{Ph}$), 125.2^a (s, *C*H$_{Im}$), 124.6^b (s, *C*H$_{Im}$), 120.7^b (d, J_{CP} = 7.1 Hz, *C*H$_{Im}$), 119.7^a (d, J_{CP} = 7.1 Hz, *C*H$_{Im}$), 68.1^b (d, $^1J_{CP}$ = 29.3 Hz, *C*HPh), 67.2^a (d, $^1J_{CP}$ = 32.3 Hz, *C*HPh), 53.8^a (d, $^3J_{CP}$ = 22.2 Hz, NCH_2), 53.7^b (d, $^3J_{CP}$ = 21.2 Hz, NCH_2), 27.0^a (d, $^2J_{CP}$ = 4.0 Hz, *C*H$_2$), 26.8^b (d, $^2J_{CP}$ = 4.0 Hz, *C*H$_2$), 25.8^a (dd, $^1J_{CP}$ = 84.8 Hz, $^2J_{CP}$ = 41.4 Hz, PC*H*), 25.5^b (dd, $^1J_{CP}$ = 85.8 Hz, $^2J_{CP}$ = 41.4 Hz, PC*H*); MS (ES$^+$): *m/z*: 749.1 [M – BF$_4$]$^+$; HRMS (ES$^+$): calcd for $C_{43}H_{37}N_2P_2Pd$, 749.1467; found, 749.1484 (ε_r = 2.3 ppm).

Synthesis of complex 15. In a glovebox, Schlenk tube was loaded with [**14**](BF$_4$) (0.040 g, 0.047 mmol) and an excess of LDA (0.035 g, 0.334 mmol). At –80 °C, THF-d_8 was added (0.7 mL). The solution then turned red instantly. After 5 min of stirring at –80 °C, the mixture was brought to RT where it was stirred for 10 min. After filtration on glass wool, the quantitative formation of complex **15** was observed by NMR. This compound was characterized by multi-nuclear NMR spectroscopy at 0 °C. ^{1}H NMR (600 MHz, THF-d_8, 0 °C): δ 7.83–7.63 (m, 10H, C*H*$_{Ph}$), 7.47–7.23 (m, 10H, C*H*$_{Ph}$), 6.95–6.85 (m, 6H, C*H*$_{Ph}$), 6.61 (d, J_{HH} = 8.4 Hz, 2H, C*H*$_{Ph}$), 6.53 (t, J_{HH} = 7.5 Hz, 2H, C*H*$_{Ph}$), 5.94 (t, J_{HH} = 6.9 Hz, 1H, C*H*$_{Ph}$), 4.12–4.06 (m, 2H, NCH_2), 2.48–2.43 (m, 1H, PC*H*), 1.78–1.73 (m, 2H, CH_2). ^{31}P{^{1}H} NMR (243 MHz, THF-d_8, 0°C): δ 30.1 (d, $^3J_{PP}$ = 14.6 Hz), 29.6 (d, $^3J_{PP}$ = 14.6 Hz). ^{13}C{^{1}H} NMR (151 MHz, THF-d_8, 0°C): δ 181.4 (dd, $^2J_{CP}$ = 34.7, 6.0 Hz, Pd−*C*$_{Ph}$), 169.4 (dd, J_{CP} = 12.1, 6.0 Hz, Pd−*C*N$_2$), 142.7 (d, J_{CP} = 6.0 Hz, *C*$_{Ph}$), 141.4 (dd, J_{CP} = 18.1, 7.5 Hz, *C*H$_{Ph}$), 140.3 (d, $^1J_{CP}$ = 119.3 Hz, *C*$_{Ph}$), 136.7 (d, $^1J_{CP}$ = 51.3 Hz, *C*$_{Ph}$), 136.4 (d, $^1J_{CP}$ = 49.8 Hz, *C*$_{Ph}$), 135.4 (d, J_{CP} = 9.1 Hz, *C*H$_{Ph}$), 134.6 (d, J_{CP} = 13.6 Hz, *C*H$_{Ph}$), 134.1 (d, J_{CP} = 9.1 Hz, *C*H$_{Ph}$), 134.0 (d, J_{CP} = 12.1 Hz, *C*H$_{Ph}$), 133.5 (d, J_{CP} = 3.0 Hz, *C*H$_{Ph}$), 132.6 (d, J_{CP} = 1.5 Hz, *C*H$_{Ph}$), 130.7 (d, J_{CP} = 21.1 Hz, *C*H$_{Ph}$), 130.5 (d, J_{CP} = 9.1 Hz, *C*H$_{Ph}$), 129.6 (brs, *C*H$_{Ph}$), 129.2 (d, J_{CP} = 3.0 Hz, *C*H$_{Ph}$), 129.1 (d, J_{CP} = 2.0 Hz, *C*H$_{Ph}$), 128.9 (d, J_{CP} = 10.6 Hz, *C*H$_{Ph}$), 128.6 (d, J_{CP} = 9.1 Hz, *C*H$_{Ph}$), 128.4 (d, J_{CP} = 10.6 Hz, *C*H$_{Ph}$), 128.1 (s, *C*H$_{Ph}$), 127.7 (d, $^1J_{CP}$ = 87.6 Hz, *C*$_{Ph}$), 124.4 (d, J_{CP} = 12.1 Hz, *C*H$_{Ph}$), 118.4 (d, J_{CP} = 12.1 Hz, *C*H$_{Ph}$), 117.5 (d, $^3J_{CP}$ = 3.0 Hz, *C*H$_{Im}$), 117.4 (s, *C*H$_{Im}$), 112.7 (s, *C*H$_{Ph}$), 68.0 (d, $^1J_{CP}$ = 83.1 Hz, P=*C*), 53.0 (d, $^3J_{CP}$ = 22.7 Hz, NCH_2), 27.6 (d, $^2J_{CP}$ = 3.0 Hz, CH$_2$), 22.6 (dd, $^1J_{CP}$ = 78.5 Hz, $^2J_{CP}$ = 39.3 Hz, PC*H*).

Synthesis of complex [16](BF$_4$). In a glovebox, Schlenk tube was loaded with [**14**](BF$_4$) (0.04 g, 0.05 mmol) and an excess of LDA (0.04 g, 0.33 mmol). At –80 °C, THF was added (2 mL) and the solution then turned red instantly. After 5 min of stirring at –80 °C, the mixture was brought to RT where it was stirred for 10 min. After returning to –80 °C, an excess of iodomethane (31 µL, 0.50 mmol) was added and the mixture was stirred for 5 min. After a pale yellow color appeared, the mixture was brought to RT and stirred for 15 min. After evaporation of the solvent and purification by chromatography on silica

(CH_2Cl_2/MeOH 99/1), complex [**16**](BF_4) was obtained as a white powder (0.035 g, 85%) and as a mixture of two diastereomers (95/5). Major isomer (95%): ^{1}H NMR (400 MHz, CD_3CN, 25 °C): δ 7.87–7.68 (m, 9H, CH_{Ph}), 7.65–7.48 (m, 10H, CH_{Ph}), 7.43 (t, J_{HH} = 8.0 Hz, 1H, CH_{Ph}), 7.26 (t, J_{HH} = 8.0 Hz, 2H, CH_{Ph}), 7.19–7.15 (m, 1H, CH_{Ph}), 7.08–6.98 (m, 2H, CH_{Ph}), 6.96–6.88 (m, 2H, CH_{Ph}), 6.84 (s, 1H, CH_{Im}), 6.70 (t, J_{HH} = 8.0 Hz, 2H, CH_{Ph}), 6.54–6.50 (m, 1H, CH_{Ph}), 4.44–4.38 (m, 1H, NCH_2), 4.08 (t, J_{HH} = 12.0 Hz, 1H, NCH_2), 3.32–3.22 (m, 1H, PCH), 2.72–2.60 (m, 1H, CH_2), 2.28–2.22 (m, 1H, CH_2), 2.22 (s, 3H, CH_3). ^{31}P{^{1}H} NMR (162 MHz, CD_3CN, 25 °C): δ 76.3 (d, $^3J_{PP}$ = 17.8 Hz, PPh_2), 32.3 (d, $^3J_{PP}$ = 17.8 Hz, $^+PPh_3$). ^{13}C{^{1}H} NMR (101 MHz, CD_3CN, 25 °C): δ 178.3 (dd, J_{CP} = 15.1, 6.1 Hz, Pd−CN_2), 176.6 (dd, $^2J_{CP}$ = 34.3, 9.1 Hz, Pd−C$_{Ph}$), 142.4 (dd, J_{CP} = 19.2, 11.1 Hz, CH_{Ph}), 141.1 (d, J_{CP} = 4.0 Hz, C$_{Ph}$), 139.2 (d, $^1J_{CP}$ = 118.2 Hz, C$_{Ph}$), 137.1 (d, J_{CP} = 14.1 Hz, CH_{Ph}), 135.0 (d, J_{CP} = 8.1 Hz, CH_{Ph}), 134.3 (d, J_{CP} = 3.0 Hz, CH_{Ph}), 134.1 (d, J_{CP} = 12.1 Hz, CH_{Ph}), 134.0 (d, J_{CP} = 10.1 Hz, CH_{Ph}), 133.7 (d, J_{CP} = 3.0 Hz, CH_{Ph}), 133.3 (s, C$_{Ph}$), 133.1 (d, J_{CP} = 3.0 Hz, CH_{Ph}), 131.9 (d, J_{CP} = 3.0 Hz, CH_{Ph}), 131.4 (d, J_{CP} = 20.2 Hz, CH_{Ph}), 130.9 (d, J_{CP} = 7.1 Hz, CH_{Ph}), 130.8 (d, $^1J_{CP}$ = 20.2 Hz, C$_{Ph}$), 130.7 (d, J_{CP} = 11.1 Hz, CH_{Ph}), 130.2 (d, J_{CP} = 9.1 Hz, CH_{Ph}), 130.1 (d, J_{CP} = 11.1 Hz, CH_{Ph}), 129.4 (d, J_{CP} = 11.1 Hz, CH_{Ph}), 128.9 (d, J_{CP} = 2.0 Hz, CH_{Ph}), 128.4 (d, J_{CP} = 2.0 Hz, CH_{Ph}), 126.5 (d, J_{CP} = 4.0 Hz, CH_{Ph}), 125.9 (d, J_{CP} = 13.1 Hz, CH_{Ph}), 124.8 (d, $^1J_{CP}$ = 39.4 Hz, C$_{Ph}$), 115.4 (d, $^3J_{CP}$ = 7.1 Hz, CH_{Im}), 69.9 (d, $^1J_{CP}$ = 30.3 Hz, C(CH_3)Ph), 50.0 (d, $^3J_{CP}$ = 24.2 Hz, NCH_2), 27.3 (d, $^2J_{CP}$ = 4.0 Hz, CH_2), 25.9 (dd, $^1J_{CP}$ = 83.8 Hz, $^2J_{CP}$ = 42.4 Hz, PCH), 22.5 (d, $^2J_{CP}$ = 3.0 Hz, C(CH_3)Ph). Minor isomer (5%): ^{1}H NMR (400 MHz, CD_3CN, 25 °C): δ 7.86–7.42 (m, 20H, CH_{Ph}), 7.29–7.24 (m, 2H, CH_{Ph}), 7.18–7.16 (m, 1H, CH_{Ph}), 7.09–7.00 (m, 3H, CH_{Ph}), 6.94–6.90 (m, 2H, CH_{Ph}), 6.70 (t, J_{HH} = 8.0 Hz, 2H, CH_{Ph}), 6.50–6.46 (m, 1H, CH_{Ar}), 4.47–4.41 (m, 1H, NCH_2), 4.31 (t, J_{HH} = 12.0 Hz, 1H, NCH_2), 3.32–3.23 (m, 1H, PCH), 2.70–2.60 (m, 1H, CH_2), 2.18–2.12 (m, 1H, CH_2), 2.14 (s, 3H, CH_3). ^{31}P{^{1}H} NMR (162 MHz, CD_3CN, 25 °C): δ 77.1 (d, $^3J_{PP}$ = 16.2 Hz, PPh_2), 32.6 (d, $^3J_{PP}$ = 16.2 Hz, $^+PPh_3$). MS (ES^+): *m/z*: 763.2 [M – BF_4]$^+$; HRMS (ES^+): calcd for $C_{44}H_{39}N_2P_2Pd$; 763.1623; found: 763.1642 (ε_r = 2.5 ppm).

Single-crystal X-ray diffraction analyses. In order to be analyzed, single crystals were coated with paratone oil and mounted onto the goniometer. The crystallographic data were obtained at 100K from a Rigaku XtaLAB Synergy diffractometer (CuKα radiation source) or from a Bruker Apex2 diffractometer (MoKα radiation source) equipped with an Oxford Cryosystem. The structures have been solved using ShelXT[31] or SUPERFLIP[32] and refined by means of least-squares procedures on F^2 or F using the program CRYSTALS.[33] The scattering factors for all the atoms were used as listed in the International Tables for X-ray Crystallography.[34] Absorption correction was performed using a Multiscan procedure.[35] Most of non-hydrogen atoms were refined anisotropically, the hydrogen atoms were located in a difference map and repositioned geometrically using a riding model. The structures [**6**]($OTf)_2$ and [**14**](BF_4) presented treated disorders on a CH_2Cl_2 and a triflate anion, respectively providing imperfect but reasonable models. Detailed crystallographic data and structural refinement parameters are given in Table S1 in the Supporting Information.

Computational Details. Geometries of isomers **15a** and **15b** were fully optimized using Gaussian 09[36] software at the PBE-D3/6-31G**/LANL2DZ* (Pd) level of calculation including *f*-polarization functions derived by Ehlers et al.[37] for Pd atom added to the LANL2DZ(Pd) basis set. Standard vibrational analysis was performed at the same calculation level to ensure that each calculated structure represents a true minimum on the potential energy surface. Gibbs free energies were calculated at 298.15 K.

Quantum Theory of Atoms In Molecules (QTAIM) analysis was performed using *AIMAll* software.[38] Topological methods are based on the analysis of the gradient field of a local function within the dynamic field theory and provide a partition of the molecular space into non-overlapping basins. The topological analysis of the electron density $\rho(r)$ designed as the by Richard Bader, yields atomic basins and QTAIM atomic charges.[39] It allows to localize so called bond paths and bond critical points (BCPs). The nature of the chemical bond is characterized from various properties of the electron density at the BCPs, namely the sign of the Laplacian of the electron density as well as the values of kinetic energy density ($\boldsymbol{G_{bcp}}$), potential energy density ($\boldsymbol{V_{bcp}}$) and total energy density $\boldsymbol{H_{bcp}} = \boldsymbol{G_{bcp}} + \boldsymbol{V_{bcp}}$, according to Bianchi's[28a] and Macchi's classifications.[40] Negative and positive values for the Laplacian at the BCP are assigned to "electron-shared" and "closed-shell" interactions, respectively.[39] According to Bianchi *et al.*[28a] the absolute ratio between the potential energy density and the kinetic energy density ($|\boldsymbol{V_{bcp}}|/\boldsymbol{G_{bcp}}$) allows distinguish three bonding situations. In particular, the intermediate bond regime ($1 < |\boldsymbol{V_{bcp}}|/\boldsymbol{G_{bcp}} < 2$) including metal-metal bonds,[41] dative bonds and weakly covalent ionic bonds is situated between electron-shared covalent bonds ($|\boldsymbol{V_{bcp}}|/\boldsymbol{G_{bcp}} > 2$) and closed-shell ionic bonds or van der Waals interactions ($|\boldsymbol{V_{bcp}}|/\boldsymbol{G_{bcp}} < 1$). The Macchi's classification offers a way to refine the bond characterization using the values of both local BCP descriptors and the delocalization index (DI). The degree of covalence for the chemical bond may be estimated from both DI and $|\boldsymbol{H_{bcp}}|/\rho_{bcp}$ ratio.[28b] The strength of the interaction may be estimated using Espinosa-Molins-Lecomte correlation[30] to give the corresponding positive interaction energy ($E_{int} = -\frac{1}{2}\mathbf{V_{bcp}}$) calculated as E_{int} (kcal.mol^{-1}) = −13.754×$\mathbf{V_{bcp}}$ (a.u.).

Electron Localization Function (ELF) topological analysis was carried out with the *TopMoD* sowtware.[42] The ELF approach measures the excess of kinetic energy arisen from Pauli repulsion[43] to provide the values between 0 and 1. ELF is close to 1 in regions where electrons are single or form antiparallel spin pairs, whereas it tends to 0 in regions with high probability to find parallel spin electrons close to one another.[43] In the area of high electron localization (atomic shells, chemical bonds and lone electron pairs) the ELF values are maximal,[44] whereas it tends to small values at the boundaries between these regions.[45] The topological analysis of the ELF gradient field provides a partition of the molecular space into non-overlapping electronic domains, so-called basins of attractors, which are classified into core, valence bonding and nonbonding basins. Depending on the symmetry, the attractors, namely local maxima of the ELF function, can be single points (general case), circles or spheres.[46] These basins are in one-to-one correspondence to the core, lone or shared pairs of the Lewis bonding model. A core basin contains a nucleus X (except a proton) and is designated as C(X). Valence bonding basins lying between two or more core basins are further distinguished by their synaptic order, defined as the number of core basins with which they share a common boundary. The monosynaptic basins denoted as V(X), correspond to lone pairs, whereas the di- and polysynaptic ones denoted as V(X1, X2, X3. ...) are related to bi- or multi-centric bonds. The average population of the basin may be calculated by the integration of the one-electron density over the basin volume. A statistical population analysis allows for considering the variance and the covariance of the basin populations being related to the electron delocalization.[47] These populations do not take integral values and are about twice the topologically defined Lewis bond orders for bonding valence basins.[48] The populations and (co)variances of these valence basins can be further interpreted in terms of weighted combinations of mesomeric structures.[47,48]

ASSOCIATED CONTENT

Supporting Information

The Supporting Information is available free of charge on the ACS Publications website.

^{1}H, ^{31}P, and ^{13}C NMR spectra for all new compounds, IR spectrum for [**6**]($OTf)_2$, and complementary crystallographic data for [**2**]Br_2, [**4**](OTf), [**6**]($OTf)_2$ and [**14**](BF_4), QTAIM charges and coordinates of the optimized structures of **15a,b** (PDF)

Accession Codes

CCDC 2283034−2283037 contains full crystallographic information for compounds unveiled in this paper. These data can be obtained free of charge via www.ccdc.cam.ac.uk/data_request/cif, or by emailing data_request@ccdc.cam.ac.uk, or by contacting The Cambridge Crystallographic Data Centre, 12 Union Road, Cambridge CB2 1EZ, UK; fax: +44 1223 336033.

AUTHOR INFORMATION

Corresponding Authors

Dmitry A. Valyaev, orcid.org/0000-0002-1772-844X; Email: dmitry.valyaev@lcc-toulouse.fr

Yves Canac, orcid.org/0000-0002-3747-554X; Email: yves.canac@lcc-toulouse.fr

Notes

The authors declare no competing financial interests.

ACKNOWLEDGMENT

The authors thank the Centre National de la Recherche Scientifique (CNRS) for financial support. R. T. and J. W. are grateful to French MENESR for a PhD fellowship. E. S. G. thanks the French Embassy in Moscow for a joint PhD scholarship (Vernadski program).

REFERENCES

(1) (a) Van Koten, G. Tuning the reactivity of metals held in a rigid ligand environment. *Pure Appl. Chem.* **1989**, *61*, 1681−1694. (b) Morales-Morales, D.; Jensen, C. G. M. *The Chemistry of Pincer Compounds*, Elsevier Science: **2011**. (c) Van Koten, G.; Milstein, D. *Organometallic Pincer Chemistry*, Eds. van Koten, G. and Milstein, D. *Top. Organomet. Chem.* **2013**, *40*, 1–356; Springer-Verlag Berlin Heidelberg.

(2) (a) *Pincer and pincer-type complexes: applications in organic synthesis and catalysis*, Eds. Szabó, K. J. and Wendt, O. F. Wiley-VCH, Weinhem, Germany, **2014**. (b) Gunanathan, G. Milstein, D. Bond activation and catalysis by ruthenium pincer complexes. *Chem. Rev.* **2014**, *114*, 12024–12087. (c) Alig, L.; Fritz, M.; Schneider, S. First-row transition metal (de)hydrogenation catalysis based on functional pincer ligands. *Chem. Rev.* **2019**, *119*, 2681−2751. (d) Kasera, A.; Biswas, J. P.; Alshehri, A. A.; Al-Thabaiti, S. A.; Mokhtar, M.; Maiti, D. Transition metal pincer complexes: a series of potential catalysts in C–H activation. *Coord. Chem. Rev*. **2023**, *475*, 214915.

(3) (a) Gallego, C. M.; Mazzeo, A.; Gaviglio, C.; Pellegrino, J.; Doctorovich, F.; Structure and reactivity of NO/NO^+/NO^- pincer and porphyrin complexes. *Eur. J. Inorg. Chem*. **2021**, *2021*, 4712–4730. (b) Wu, S.; Wu, Z.; Ge, Q.; Zheng, X.; Yang, Z. Antitumor activity of tridentate pincer and related metal complexes. *Org. Biomol. Chem*. **2021**, *19*, 5254–5273.

(4) (a) Hawk, J. L.; Craig, S. L. Physical and materials applications of pincer complexes. *Top. Organomet. Chem*. **2013**, *40*, 319–352. (b) Haque, A.; Xu, L.; Al-Balushi, R. A.; Al-Suti, M. K.; Ilmi, R.; Guo, Z.; Khan, M. S.; Wong, W.-Y.; Raithby, P. R. Cyclometallated tridentate platinum(II) arylacetylide complexes: old wine in new bottles. *Chem. Soc. Rev.* **2019**, *48*, 5547−5563. (c) Kocherga, M.; Boyle, K. M.; Merkert, J.; Schmedake, T. A.; Walter, M. G. Exploring the molecular electronic device applications of synthetically versatile silicon pincer complexes as charge transport and electroluminescent layers. *Mater. Adv*. **2022**, *3*, 2373–2379.

(5) Moulton, C. J.; Shaw, B. L. Transition metal-carbon bonds. Part XLII. Complexes of nickel, palladium, platinum, rhodium and iridium with the tridentate ligand 2,6-bis[(di-t-butylphosphino)methyl]phenyl. *J. Chem. Soc., Dalton Trans.* **1976**, 1020–1024.

(6) Van Koten, G.; Timmer, K.; Noltes, J. G.; Spek, A. L. A novel type of Pt–C interaction and a model for the final stage in reductive elimination processes involving C–C coupling at Pt; synthesis and molecular geometry of [1,*N*,*N*'-η-2,6-bis{(dimethylamino)methyl}toluene]iodoplatinum(II) tetrafluoroborate. *J. Chem. Soc., Chem. Comm*. **1978**, 250–252.

(7) (a) Murugesan, S.; Kirchner, K. Non-precious metal complexes with an anionic PCP pincer architecture. *Dalton Trans*. **2016**, *45*, 416–439. (b) van der Vlugt, J. I.; Reek, J. N. H. Neutral tridentate PNP ligands and their hybrid analogues: versatile non-innocent scaffolds for homogeneous catalysis. *Angew. Chem. Int. Ed.* **2009**, *48*, 8832−8846. (c) Adams, G. M.; Weller, A. S. POP-type ligands: variable coordination and hemilabile behaviour. *Coord. Chem. Rev*. **2018**, *355*, 150–172.

(8) (a) Yang, L.; Zhang, X.; Mao, P.; Xiao, Y.; Bian, H.; Yuan, J.; Mai, W.; Qu, L. NCN pincer palladium complexes based on 1,3-dipicolyl-3,4,5,6-tetrahydropyrimidin-2-ylidenes: synthesis, characterization and catalytic activities. *RSC Adv*. **2015**, *5*, 25723–25729. (b) González-Sebastián, L.; Canseco-Sebastián, D.; Morales-Morales, D. Benzene-derived organometallic pincer compounds bearing six-membered metallacycles and up. *Pincer Compounds: Chemistry and applications*, Elsevier **2018**, 467–490.

(9) (a) Naghipour, A.; Sabounchei, S. J.; Morales-Morales, D.; Canseco-González, D.; Jensen, C. M. A highly active two-six membered phosphinite palladium PCP pincer complex [PdCl{$C_6H_3(CH_2OPPr^i)_2$-2,6}]. *Polyhedron* **2007**, *26*, 1445–1448. (b) Yoon, M. S.; Ryu, D.; Kim, J.; Ahn, K. H. Palladium pincer complexes with reduced bond angle strain: efficient catalysts for the Heck reaction. *Organometallics* **2006**, *25*, 2409–2411.

(10) Asay, M.; Morales-Morales, D. Non-symmetric pincer ligands: complexes and application in catalysis. *Dalton Trans*. **2015**, *44*, 17432–17447.

(11) (a) Eberhard, M. R.; Matsukawa, S.; Yamamoto, Y.; Jensen, C. M. Novel unsymmetrical PCP' pincer ligands and their palladium(II) complexes. *J. Organomet. Chem*. **2003**, *687*, 185–189. (b) Abrahamsson, M.; Wolpher, H.; Johansson, O.; Larsson, J.; Kritikos, M.; Eriksson, L.; Norrby, P.-O.; Bergquist, J.; Sun, L.; Åkermark, B.; Hammarström, L. A new strategy for the improvement of photophysical properties in ruthenium(II) polypyridyl complexes. Synthesis and photophysical and electrochemical characterization of six mononuclear ruthenium(II) bisterpyridine-type complexes. *Inorg. Chem.* **2005**, *44*, 3215–3225. (c) Kozlov, V. A.; Aleksanyan, D. V.; Nelyubina, Yu. V.; Lyssenko, K. A.; Gutsul, E. I.; Vasil'ev, A. A.; Petrovskii, P. V.; Odinets, I. L. 5,6-Membered palladium pincer complexes of 1-thiophosphoryloxy-3-thiophosphorylbenzenes. Synthesis, X-ray structure, and catalytic activity. *Dalton Trans*. **2009**, 8657−8666. (d) Churusova, S. G.; Aleksanyan, D. V.; Rybalkina, E. Y.; Susova, O. Y.; Brunova, V. V.; Aysin, R. R.; Nelyubina, Yu. V.; Peregudov, A. S.; Gutsul, E. I.; Klemenkova, Z. S.; Kozlov, V. A. Highly cytotoxic palladium(II) pincer complexes based on picolinylamides functionalized with amino acids bearing ancillary *S*-donor groups. *Inorg. Chem*. **2017**, *56*, 9834−9850. (e) Sinha, N. K.; Thirupathi, N. [6,5] CNN palladium(II) pincer complexes containing *N*-substituted monoanionic and dianionic guanidinate ligands: syntheses, structural aspects, and their utility in Suzuki-Miyaura coupling reactions. *Organometallics* **2021**, *40*, 3535−3549. (f) Buhaibeh, R.; Duhayon, C.; Valyaev, D. A.; Sortais, J.-B.; Canac, Y. Cationic PCP and PCN NHC core pincer-type Mn(I) complexes: from synthesis to catalysis. *Organometallics* **2021**, *40*, 231−241.

(12) (a) Peris, E.; Crabtree, R. H. Key factors in pincer ligand design. *Chem. Soc. Rev*. **2018**, *47*, 1959−1968. (b) Castro-Rodrigo, R.; Esteruelas, M. A.; Gómez-Bautista, D.; Lezáun, V.; López, A. M.; Oliván, M; Oñate, E. Influence of the bite angle of dianionic C,N,C-pincer ligands on the chemical and photophysiscal properties of iridium(III) and osmium(IV) hydride complexes. *Organometallics* **2019**, *38*, 3707−3718.

(13) (a) Peris, E.; Loch, J. A.; Mata, J.; Crabtree, R. H. A Pd complex of a tridentate pincer CNC bis-carbene ligand as a robust homogeneous Heck catalyst. *Chem. Commun*. **2001**, 201−202. (b) Tulloch, A. A. D.; Danopoulos, A. A.; Tizzard, G. J.; Coles, S. J.; Hursthouse, M. B.; Hay-Motherwell, R. S.; Motherwell, W. B. Chiral 2,6-lutidinyl-biscarbene complexes of palladium. *Chem. Commun*. **2001**, 1270−1271. (c) Hahn, F. E.; Jahnke, M. C.; Pape, T. Synthesis of palladium and platinum complexes with phosphine-functionalized benzimidazolin-2-ylidene ligands. *Organometallics*, **2006**, *25*, 5927−5936. (d) Andrew, R. E.; González-Sebastián, L.; Chaplin, A. B. NHC-based pincer ligands: carbenes with a bite. *Dalton Trans*. **2016**, *45*, 1299−1305. (e) Taakili, R. Canac, Y. NHC core pincer ligands exhibiting two anionic coordinating extremities. *Molecules* **2020**, *25*, 2231. (f) Wang, Y.; Zhang, B.; Guo, S. Transition metal complexes supported by N-Heterocyclic carbene-based pincer platforms: synthesis, reactivity and applications. *Eur. J. Inorg. Chem*. **2021**, *2021*, 188−204.

(14) For examples with group 10 transition metals, see: (a) Vabre, B.; Canac, Y.; Duhayon, C.; Chauvin, R.; Zargarian, D. Nickel(II) complexes of the new pincer-type unsymmetrical ligands PIMCOP,

PIMIOCOP, and NHCCOP: versatile binding motifs. *Chem. Commun*. **2012**, *48*, 10446−10448. (b) Vabre, B.; Canac, Y.; Lepetit, C.; Duhayon, C.; Chauvin, R.; Zargarian, D. Charge effects in PCP pincer complexes of Ni^{II} bearing phosphinite and imidazol(i)ophosphine coordinating jaws: from synthesis to catalysis through bonding analysis. *Chem. Eur. J*. **2015**, *21*, 17403−17414. (c) Therrien, J. A.; Wolf, M. O. The influence of *para* substituents in bis(N-Heterocyclic carbene) palladium pincer complexes for electrocatalytic CO_2 reduction. *Inorg. Chem*. **2017**, *56*, 1161−1172. (d) Burks, D. B.; Davis, S.; Lamb, R. W.; Liu, X.; Rodrigues, R. R.; Liyanage, N. P.; Sun, Y.; Webster, C. E.; Delcamp, J. H.; Papish, E. T. Nickel(II) pincer complexes demonstrate that the remote substituent controls catalytic carbon dioxide reduction. *Chem. Commun*. **2018**, *54*, 3819−3822.

(15) For examples with group 10 transition metals, see: (a) Borré, E.; Dahm, G.; Aliprandi, A.; Mauro, M.; Dagorne, S.; Bellemin-Laponnaz, S. Tridentate complexes of group 10 bearing bis-aryloxide N-heterocyclic carbene ligands: synthesis, structural, spectroscopic, and computational characterization. *Organometallics* **2014**, *33*, 4374−4384. (b) Nair, A. G.; McBurney, R. T.; Gatus, M. R. D.; Walker, D. B.; Bhadbhade, M.; Messerle, B. A. Synthesis and catalytic activity of nickel(II)complexes containing NCN pincer ligands. J. *Organomet. Chem.* **2017**, *845*, 63−70. (c) Subramaniyan, V.; Dutta, B.; Govindaraj, A.; Mani, G. Facile synthesis of Pd(II) and Ni(II) pincer carbene complexes by the double C−H bond activation of a new hexahydropyrimidine-based bis(phosphine): catalysis of C−N couplings. *Dalton Trans*. **2019**, *48*, 7203−7210.

(16) (a) Taakili, R.; Lepetit, C.; Duhayon, C.; Valyaev, D. A.; Lugan, N.; Canac, Y. Palladium(II) pincer complexes of a *C,C,C*-NHC, diphosphonium bis(ylide) ligand. *Dalton Trans*. **2019**, *48*, 1709−1721. (b) El Kadiri, M.; Chihab, A.; Taakili, R.; Duhayon, C.; Valyaev, D. A.; Canac, Y. Diverse *C*-coordination modes of NHC-tricyclohexylphosphonium ylide ligands in palladium(II) complexes. *Organometallics* **2022**, *41*, 456–466.

(17) Taakili, R.; Barthes, C.; Goëffon, A.; Lepetit, C.; Duhayon, C.; Valyaev, D. A.; Canac, Y. NHC core phosphonium ylide-based palladium(II) pincer complexes: the second ylide extremity makes the difference. *Inorg. Chem*. **2020**, *59*, 7082–7096.

(18) (a) Canac, Y. Carbeniophosphines versus phosphoniocarbenes: the role of the positive charge. *Chem. Asian. J.* **2018**, *13*, 1872−1887. (b) Valyaev, D. A.; Canac, Y. Carbenes and phosphonium ylides: a fruitful association in coordination chemistry. *Dalton Trans*. **2021**, *50*, 16434−16442. (c) Canac, Y. Carbon-phosphorus ligands with extreme donating character. *Chem. Record.* **2023**, e202300187.

(19) (a) Schmidbaur, H. Phosphorus ylides in the coordination sphere of transition metals: an inventory. *Angew. Chem. Int. Ed. Engl*. **1983**, *22*, 907–927. (b) Kaska, W. C.; Ostoja Starzewski, K. A, in: *Ylides and Imines of Phosphorus*; Johnson, A. W., Eds, John Wiley & Sons: New York, **1993**, chapter 14. (c) Urriolabeitia, E. P. sp^3-hybridized neutral η^1-carbon ligands. *Top. Organomet. Chem.* Chauvin, R.; Canac, Y. Eds, Springer, **2010**, *30*, 15–48. (d) Shi, Y.; Pan, B-W.; Yu, J-S.; Zhou, Y.; Zhou, J. Recent advances in applying carbonyl-stabilized phosphorus ylides for catalysis. *ChemCatChem* **2021**, *13*, 129–139.

(20) (a) Fenske, D.; Brandt, K.; Stock, P. Unusual reaction of (σ-allyl)manganesepentacarbonyl with bis(diphenylphosphino)-N-methyl maleic anhydride. *Z. Naturforsch.* **1981**, *36b*, 768−770. (b) Lorenz, I. P.; Pohl, W.; Nöth H.; Schmidt, M. *P*-Funktionalisierte diferriophosphonium salze des typs $[\{CpFe(CO)_2\}_2PPhR]^+X^-$ und $[\{CpFe(CO)_2\}_2PClR]^+X^-$. *J. Organomet. Chem*. **1994**, *475*, 211−221. (c) Nakajima, Y.; Ozawa, F. Redox chemistry of bis(phosphaethenyl)pyridine iron complexes. *Organometallics* **2012**, *31*, 2009−2015.

(21) CCDC 2283034−2283037 contains full crystallographic information for compounds [**2**]Br_2, [**4**](OTf), [**6**](OTf)$_2$ and [**14**](BF$_4$). These data can be obtained free of charge from the Cambridge Crystallographic Data Centre via www.ccdc.cam.ac.uk/data_request/cif.

(22) Li, Y.; Lu, L.-Q.; Das, S.; Pisiewicz, S.; Junge, K.; Beller, M. Highly chemoselective metal-free reduction of phosphine oxides to phosphines. *J. Am. Chem. Soc.* **2012**, *134*, 18325–18329.

(23) Taakili, R.; Barthes, C.; Lepetit, C.; Duhayon, C.; Valyaev, D. A.; Canac, Y. Direct access to palladium(II) complexes based on anionic *C,C,C*-phosphonium ylide core pincer ligand. *Inorg. Chem.* **2021**, *60*, 12116–12128.

(24) (a) Valyaev, D. A.; Filippov, O. A.; Lugan, N.; Lavigne, G. Ustynyuk, N. A. Umpolung of methylenephosphonium ions in their manganese half-sandwich complexes and applications to the synthesis of chiral phosphorus-containing ligand scaffolds. *Angew. Chem. Int. Ed.* **2015**, *54*, 6315−6319. (b) Valyaev, D. A.; Willot, J.; Mangin, L. P.; Zargarian, D.; Lugan, N. Manganese-mediated synthesis of an NHC core non-symmetric pincer ligand and evaluation of its coordination properties. *Dalton. Trans*. **2017**, *46*, 10193−10196.

(25) Valyaev, D. A.; Bastin, S.; Utegenov, K. I.; Lugan, N.; Lavigne, G.; Ustynyuk, N. A. A direct, modular and efficient construction of the P–C–P structural motif *via* coupling of manganese carbyne complexes with phosphines. *Chem. Eur. J.* **2014**, *20*, 2175−2178.

(26) Buhaibeh, R.; Filippov, O. A.; Bruneau-Voisine, A.; Willot, J.; Duhayon, C.; Valyaev, D. A.; Lugan, N.; Canac, Y.; Sortais, J. B. Phosphine-NHC manganese hydrogenation catalyst exhibiting a non-classical metal-ligand cooperative H_2 activation mode. *Angew. Chem. Int. Ed.* **2019**, *58*, 6727–6731.

(27) Yang, L.; Powell, D. R.; Houser, R. P. Structural variation in copper(I) complexes with pyridylmethylamide ligands: structural analysis with a new four-coordinate geometry index, τ4. *Dalton Trans*. **2007**, 955–964.

(28) (a) Bianchi, R.; Gervasio, G.; Marabello, D. Experimental electron density analysis of $Mn_2(CO)_{10}$: metal-metal and metal-ligand bond characterization. *Inorg. Chem.* **2000**, *39*, 2360−2366. (b) Espinosa, E.; Alkorta, I.; Elguero, J.; Molins, E. From weak to strong interactions: a comprehensive analysis of the topological and energetic properties of the electron density distribution involving X-HF-Y systems. *J. Chem. Phys*. **2002**, 117, 5529−5542.

(29) Lepetit, C.; Vabre, B.; Canac, Y.; Esmaïl Alikhani, M.; Zargarian, D. Pentacoordinated, square pyramidal cationic PCP Ni(II) pincer complexes: ELF and QTAIM topological analyses of nickel-triflate interactions. *Theor. Chem. Acc*. **2018**, *137*, 141.

(30) (a) Espinosa, E.; Molins, E.; Lecomte C. Hydrogen bond strengths revealed by topological analyses of experimentally observed electron densities *Chem. Phys. Lett*. **1998**, *285*, 170–173. (b) Espinosa, E.; Alkorta, I.; Rozas, I.; Elguero, J.; Molins E. About the evaluation of the local kinetic, potential and total energy densities in closed-shell interactions. *Chem. Phys. Lett*. **2001**, *336*, 457–461.

(31) Sheldrick, G. M. SHELXT - Integrated space-group and crystal-structure determination, *Acta Cryst*. **2015**, *A71*, 3−8.

(32) Palatinus, L.; Chapuis, G. Superflip – a computer program for the solution of crystal structures by charge flipping in arbitrary dimensions. *J. Appl. Cryst*. **2007**, *40*, 786−790.

(33) Betteridge, P. W.; Carruthers, J. R.; Cooper, R. I.; Prout, K.; Watkin, D. J. CRYSTALS version 12: software for guided crystal structure analysis. *J. Appl. Cryst.* **2003**, *36*, 1487.

(34) Sheldrick, G. M. A short history of SHELX. *Acta Cryst*. **2008**, *A64*, 112−122.

(35) Blessing, R. H. An empirical correction for absorption anisotropy. *Acta Cryst*. **1995**, *A51*, 33−38.

(36) *Gaussian 09, Revision D.01*, M. J. Frisch, G. W. Trucks, H. B. Schlegel, G. E. Scuseria, M. A. Robb, J. R. Cheeseman, G. Scalmani, V. Barone, B. Mennucci, G. A. Petersson, H. Nakatsuji, M. Caricato, X. Li, H. P. Hratchian, A. F. Izmaylov, J. Bloino, G. Zheng, J. L. Sonnenberg, M. Hada, M. Ehara, K. Toyota, R. Fukuda, J. Hasegawa, M. Ishida, T. Nakajima, Y. Honda, O. Kitao, H. Nakai, T. Vreven, J. A. Montgomery, Jr., J. E. Peralta, F. Ogliaro, M. Bearpark, J. J. Heyd, E. Brothers, K. N. Kudin, V. N. Staroverov, R. Kobayashi, J. Normand, K. Raghavachari, A. Rendell, J. C. Burant, S. S. Iyengar, J. Tomasi, M. Cossi, N. Rega, J. M. Millam, M. Klene, J. E. Knox, J. B. Cross, V. Bakken, C. Adamo, J. Jaramillo, R. Gomperts, R. E. Stratmann, O. Yazyev, A. J. Austin, R. Cammi, C. Pomelli, J. W. Ochterski, R. L. Martin, K. Morokuma, V. G. Zakrzewski, G. A. Voth, P. Salvador, J. J. Dannenberg, S. Dapprich, A. D. Daniels, Ö. Farkas, J. B. Foresman, J. V. Ortiz, J. Cioslowski, and D. J. Fox, Gaussian, Inc., Wallingford CT, **2009**.

(37) Ehlers, A.W.; Böhme, M.; Dapprich, S.; Gobbi, A.; Höllwarth, A.; Jonas, V.; Köhler, K. F.; Stegmann, R.; Veldkamp, A.; Frenking, G. A set of f-polarization functions for pseudo-potential basis sets of the transition metals Sc-Cu, Y-Ag and La-Au. *Chem. Phys. Lett.* **1993**, *208*, 111−114.

(38) Keith, T. A. *AIMAll (Version 17.11.14)*, TK Gristmill Software, Overland Park KS, USA, **2017**, aim.tkgristmill.com

(39) (a) Bader, R. F. W. in *Atoms In Molecules*, **1990**, Clarendon Press: Oxford, UK. (b) Bader, R. F. W.; Essen, H. The characterization of atomic interactions. *J. Chem. Phys.* **1984**, *80*, 1943−1960.

(40) Macchi, P.; Proserpio, D. M.; Sironi, A. Experimental electron density in a transition metal dimer: metal-metal and metal-ligand Bonds. *J. Am. Chem. Soc.* **1998**, *120*, 13429−13435.

(41) Lepetit, C.; Fau, P.; Fajerwerg, K.; Kahn, M. L.; Silvi, B. Topological analysis of the metal-metal bond: a tutorial review. *Coord. Chem. Rev*. **2017**, *345,* 150−181.

(42) Noury, S.; Krokidis, X.; Fuster, F.; Silvi, B. Computational tools for the electron localization function topological analysis. *Comput. & Chem.* **1999**, *23*, 597−604.

(43) (a) Becke, A. D.; Edgecombe, K. E. A simple measure of electron localization in atomic and molecular systems. *J. Chem. Phys*. **1990**, *92*, 5397−5403. (b) Silvi, B.; Savin, A. Classification of chemical bonds based on topological analysis of electron localization function. *Nature* **1994***, 371*, 683–686.

(44) Poater, J.; Duran, M.; Solà, M.; Silvi, B. Theoretical evaluation of electron delocalization in aromatic molecules by means of atoms in molecules (AIM) and electron localization function (ELF) topological approaches. *Chem. Rev.* **2005**, *105*, 3911–3947.

(45) Silvi. B.; Gillespie, R. J., Gatti, C. in Comprehensive Inorganic Chemistry II. **2013**, *9*, 187–226.

(46) Silvi, B.; Fourré, I.; Alikhani, M. E. The topological analysis of the electron localization function. A key for a position space representation of chemical bonds. *Monat. Chem.* **2005**, *136*, 855–879.

(47) Silvi, B. How topological partitions of the electron distributions reveal delocalization. *Phys. Chem. Chem. Phys*. **2004**, *6*, 256–260.

(48) Lepetit, C.; Silvi, B.; Chauvin, R. ELF analysis of out-of-plane aromaticity and in-plane homoaromaticity in carbo[*N*]annulenes and [*N*]pericyclynes. *J. Phys. Chem. A* **2003**, *107*, 464–473.

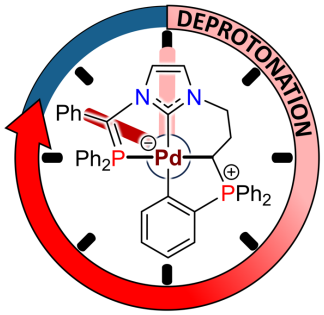

Table of Contents artwork

Incorporation of phenyl substituent into the bridge between phosphine and NHC moieties in phosphine-NHC-ylide precursor allows to access unique zwitterionic Pd(II) complex exhibiting two different types of phosphonium ylide ligands *via* four consecutive C−H deprotonation steps